

# A Critical Approach to the Thermodynamic Characterization of Inclusion Complexes: Multiple-Temperature Isothermal Titration Calorimetric Studies of Native Cyclodextrins with Sodium Dodecyl Sulfate

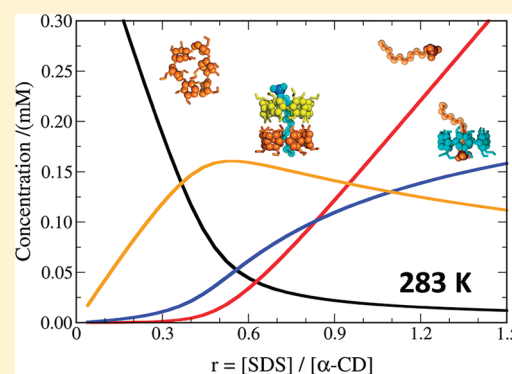
Pilar Brocos,<sup>†</sup> Xavier Banquy,<sup>‡,§</sup> Norma Díaz-Vergara,<sup>‡,||</sup> Silvia Pérez-Casas,<sup>‡</sup> Ángel Piñeiro,<sup>\*,†,‡</sup> and Miguel Costas<sup>\*,‡</sup>

<sup>†</sup>Departamento de Física Aplicada, Facultad de Física, Universidad de Santiago de Compostela, Campus Vida, E-15782 Santiago de Compostela, Spain

<sup>‡</sup>Laboratorio de Biofísicoquímica, Departamento de Físicoquímica, Facultad de Química, Universidad Nacional Autónoma de México, Cd. Universitaria, México D.F. 04510, Mexico

## S Supporting Information

**ABSTRACT:** Inclusion complexes based on native cyclodextrins are basic building blocks for the design of a new generation of promising materials. The design process can be optimized by maximizing the population of the desired chemical species. This is greatly facilitated by an accurate characterization of the thermodynamic parameters for their formation. A critically assessed literature review of equilibrium constants for cyclodextrin:sodium dodecyl sulfate (CD:SDS) complexes is reported. We performed multiple-temperature isothermal titration calorimetric (283–323 K) measurements for these systems, leading to the first reported heat capacity changes of binding. Data were analyzed using two thermodynamic models by homemade programs that also provide the distribution of chemical species as a function of the experimental variables. Assisted by earlier molecular dynamic simulations, a microscopic-level discussion of the contributions to the thermodynamic parameters is given. On the basis of our results, a number of recommendations to obtain reliable association parameters for CD-based inclusion complexes are listed.



## 1. INTRODUCTION

Native cyclodextrins are short cyclic polysaccharides that consist of six ( $\alpha$ -CD), seven ( $\beta$ -CD), or eight ( $\gamma$ -CD)  $\alpha$ -D-glucopyranoside rings, whose geometry is roughly that of empty truncated cones. Their unique topology confers them peculiar physicochemical properties that have allowed their application in different fields.<sup>1</sup> For example, because the internal part of the CDs is more hydrophobic than their external surface, they are able to host hydrophobic molecules, thus increasing their solubility in water.<sup>2</sup> This feature has been exploited to transport and/or protect hydrophobic or amphiphilic compounds in aqueous media.<sup>3</sup> The ability of CDs and CD-based complexes to self-assemble is currently being explored as an alternative for the design of new materials with interesting properties for potential applications to a number of fields.<sup>4–17</sup> A large body of information in the literature indicates that, as a consequence of their high stability, biocompatibility, low toxicity, and versatility (relatively small chemical modifications produce significant changes in the physicochemical properties), cyclodextrins are attractive candidates for further development of a wide variety of applications.

Recently, we have reported the formation of ( $\alpha$ -CD)-based tubular structures spontaneously formed at the air/water interface

that, in the presence of the sodium dodecyl sulfate (SDS), acquire a surprisingly high viscoelasticity.<sup>4,18</sup> These films could have potential applications in separation membrane systems, specific coatings, and biosensing devices. The viscoelasticity of  $\alpha$ -CD+SDS films strongly depends on the relative concentration of  $\alpha$ -CD and SDS in the bulk solution, as well as on the temperature. It was suggested that the adsorption of 2:1 complexes to the air/water interface might be responsible for the film high viscoelasticity.<sup>4</sup> Work by Jiang et al.<sup>6</sup> also explains the formation of vesicles and of more intricate structures like annular-ring microtubes<sup>5</sup> by the self-assembly of 2:1 complexes based on  $\beta$ -CD and SDS. In general, aqueous solutions of CDs and SDS might contain five or six different chemical species including the free molecules and the 1:1, 2:1, 1:2, and 2:2 complexes. The concentration of each species depends on the temperature and the relative concentration of both solutes, as well as on the particular CD being used, the pH, the absence or presence of salt, etc. As it seems that 2:1 inclusion complexes are

**Received:** September 9, 2011

**Revised:** October 18, 2011

**Published:** October 20, 2011

the building blocks for the formation of larger structures, which, in turn, might be key for the design of new materials, it is important to characterize in detail the thermodynamic parameters for their formation. This would allow optimizing the design process by working at the experimental conditions that maximize the population of the desired chemical species, bearing in mind that the chemical equilibria with other species could hinder the control of the target structure or the required task. The detailed and critically assessed literature review reported here shows that the thermodynamic characterization for the formation of CD:SDS inclusion complexes has not been achieved yet. In fact, there are a large number of widely different values for the equilibrium constants characterizing the formation of each species. This was noted by Mwakibete et al.,<sup>19</sup> who proposed a two-class categorization of experimental techniques to address this problem. Such lack of consistency is extended to other thermodynamic properties like the enthalpy of formation and the complex stoichiometry. This situation encouraged us to perform a comprehensive study of the mixtures formed by each of the three native CDs and SDS at three levels. First, we carried out a large set of isothermal titration calorimetric (ITC) measurements at different temperatures; the choice of ITC was based on the fact that it is recognized as a reference technique for thermodynamic characterization of complex formation. Second, we performed a detailed analysis of the data using both commercial software and homemade programs with two of the most commonly employed thermodynamical models for binding studies. Third, we further analyzed earlier molecular dynamic simulations<sup>20</sup> to support a detailed discussion at the molecular level of the different contributions to the thermodynamic parameters. Because our approach to the study of CD:SDS mixtures can be extended to other systems, a number of recommendations to obtain reliable association parameters for CD-based inclusion complexes are also given.

## 2. MATERIALS AND METHODS

**2.1. Materials.** Sodium dodecyl sulfate (99.0%) was obtained from Fluka.  $\beta$ -Cyclodextrin (>98%) and  $\alpha$ -cyclodextrin (>98%) were purchased from Sigma-Aldrich, while  $\gamma$ -cyclodextrin (>99%) was a generous gift from Cerestar (Cargill Co., USA). The CD water content was determined by Karl Fisher titration (701 KF Titrino, Metrohm, Switzerland) giving the following results (% w/w): 10.92 for  $\alpha$ -CD, 12.36 for  $\beta$ -CD, and 10.71 for  $\gamma$ -CD. All chemicals were used without further purification. Water was distilled and deionized using a Barnstead Nanopure Infinity equipment, its resistivity being  $18.0 \pm 0.2 \text{ M}\Omega \text{ cm}^{-1}$ . Prior to use, it was degassed. The solutions were carefully prepared by mass (Mettler AT250 balance, Switzerland) taking into account the water content of each CD.

**2.2. Calorimetry.** **2.2.1. Experimental Procedure.** Isothermal titration calorimetry experiments were performed on a VP-ITC microcalorimeter (MicroCal Inc., Northampton, U.S.). A detailed description of this power-compensation calorimeter can be found elsewhere.<sup>21</sup> It was calibrated by dissipating a known power through a resistive heater in contact with the measurement cell wall. Typical binding isotherms were obtained by filling the syringe (296  $\mu\text{L}$ ) with the surfactant solution ( $\sim 5 \text{ mM}$ ) and the sample cell (1.4166 mL) with the CD solution ( $\sim 0.45 \text{ mM}$  after water-content correction). To obtain a better signal-to-noise ratio, the procedure was reversed in the case of  $\gamma$ -cyclodextrin

systems; that is, the  $\gamma$ -CD solution ( $\sim 4.5 \text{ mM}$ ) was placed in the syringe and the SDS solution ( $\sim 0.5 \text{ mM}$ ) in the sample cell. In all cases, the SDS concentration was much lower than its critical micelle concentration over the entire temperature range studied (the  $\text{cmc}(T)$  for SDS is a parabola-shaped curve with a minimum at  $\sim 8 \text{ mM}$  in the range [292, 303] K as determined by different techniques).<sup>22,23</sup> Initial equilibration time before starting each experiment was set to 1 h to ensure the stability of the power baseline. Injections of 5 or 10  $\mu\text{L}$  at a constant rate of  $0.5 \mu\text{L s}^{-1}$  were performed every 10 min (the 10  $\mu\text{L}$  injections applied for runs involving  $\beta$ -CD at  $T \geq 313.15 \text{ K}$  and  $\gamma$ -CD). The solution in the measurement cell was kept in constant stirring at 450 rpm during the experiments. Care was taken to set the reference power of the ITC apparatus to a high enough value, typically of the order of  $40 \mu\text{J s}^{-1}$ , to avoid negative signals. In this way, it was ensured that the observed signal was not disturbed by any power overcompensation from the controller. The experiments corresponding to the dilution of SDS were also performed at each working temperature; that is, the surfactant solution was placed in the syringe, and the sample cell was filled with pure water. In the CD dilution experiments, no calorimetric signal was detected. Hence, the difference between the signals obtained with the  $\alpha$ - or  $\beta$ -CD solution and with pure water in the sample cell afforded the signal specifically associated with the binding process. Experiments involving  $\gamma$ -CD solution titrations with a SDS solution in the sample cell were directly employed to determine the corresponding binding isotherms due to the negligible heat associated with the slight dilution of SDS during these experiments. It was verified that the pH of the solutions was not significantly affected by the concentration change produced during the titration process. Following the described procedure, experiments were performed for the three cyclodextrins at various temperatures between 283 and 323 K.

**2.2.2. Analysis.** To analyze the binding isotherms, a Sequential Binding Sites (SBS) model allowing for  $A_1B_1$ ,  $A_1B_2$ , and  $A_2B_1$  species was considered. Higher-order complexes were discarded, because they would involve more parameters with no significant improvement of the fittings to the experimental data. Because of its recurrent occurrence in the literature, the ability of the Single Set of Identical Sites (SSIS) model<sup>21,24–28</sup> to describe the  $\beta$ -CD:SDS systems was also evaluated (see Appendix in the Supporting Information).

**SBS Model.** We keep restricted to a particular case ( $A_mB_n$  complexes, with  $m, n \leq 2$  and  $m + n \leq 3$ ) of a generic model in which A and B are simultaneously visualized as molecules with any number of binding sites and as potential ligands. Its specific formulation in the framework of isothermal titration calorimetry is based on the cumulative heat involved in the mixing of A and B in the sample cell of the calorimeter at the total concentrations  $[A]_j$  and  $[B]_j$  after  $j$  titrations:

$$Q_j^{\text{cum}} = \sum_{i=1}^j Q_i = [A]_j V_0 [A_{11} \Delta H_{11}^\circ + A_{12} (\Delta H_{11}^\circ + \Delta H_{12}^\circ) + (1/2) A_{21} (\Delta H_{11}^\circ + \Delta H_{21}^\circ)] \\ = [B]_j V_0 [B_{11} \Delta H_{11}^\circ + (1/2) B_{12} (\Delta H_{11}^\circ + \Delta H_{12}^\circ) + B_{21} (\Delta H_{11}^\circ + \Delta H_{21}^\circ)] \quad (1)$$

where  $Q_i$  is the heat associated with each titration and  $V_0$  is the effective volume of the cell, whereas  $A_{mn}$  and  $B_{mn}$  are the fractions of A and B molecules, respectively, involved in

$A_m B_n$  species,

$$\begin{aligned} A_{10} &= \frac{1}{S_A}; A_{11} = \frac{K_{11}[B_f]_j}{S_A}; A_{12} = \frac{K_{11}K_{12}[B_f]_j^2}{S_A}; A_{21} = \frac{2K_{11}K_{21}[A_f]_j[B_f]_j}{S_A} \\ B_{01} &= \frac{1}{S_B}; B_{11} = \frac{K_{11}[A_f]_j}{S_B}; B_{21} = \frac{K_{11}K_{21}[A_f]_j^2}{S_B}; B_{12} = \frac{2K_{11}K_{12}[A_f]_j[B_f]_j}{S_B} \end{aligned} \quad (2)$$

that are obtained from the corresponding binding polynomials<sup>29</sup>  $S_A$  and  $S_B$ :

$$\begin{aligned} \left(\sum_{n=0}^2 A_{1n}\right) + A_{21} &= 1 \Leftrightarrow S_A = 1 + K_{11}[B_f]_j + K_{11}K_{12}[B_f]_j^2 \\ &\quad + 2K_{11}K_{21}[A_f]_j[B_f]_j \\ \left(\sum_{m=0}^2 B_{m1}\right) + B_{12} &= 1 \Leftrightarrow S_B = 1 + K_{11}[A_f]_j + K_{11}K_{21}[A_f]_j^2 \\ &\quad + 2K_{11}K_{12}[A_f]_j[B_f]_j \end{aligned} \quad (3)$$

In this context,  $[A_f]_j$  and  $[B_f]_j$  stand for the concentration of free A and B molecules after  $j$  titrations and are related to  $[A]_j$  and  $[B]_j$  as follows:

$$\begin{aligned} [B]_j &= [B_f]_j + [A]_j \sum_{\substack{m,n=1 \\ m+n \leq 3}}^2 (n/m)A_{mn}; \\ [A]_j &= [A_f]_j + [B]_j \sum_{\substack{m,n=1 \\ m+n \leq 3}}^2 (m/n)B_{mn} \end{aligned} \quad (4)$$

where the sum in the first (second) expression represents the average number of B (A) molecules bound per A (B) molecule. In eqs 1–3,  $K_{1n}$  and  $\Delta H_{1n}^\circ$  denote the stepwise equilibrium constant and binding enthalpy associated with the process  $A_1 B_{n-1} + B \rightleftharpoons A_1 B_n$ , while  $K_{m1}$  and  $\Delta H_{m1}^\circ$  are the corresponding quantities for the process  $A_{m-1} B_1 + A \rightleftharpoons A_m B_1$ . This model has been successfully applied in the past to cyclodextrin–surfactant systems.<sup>30</sup> A simplified version, in which A is a molecule with two binding sites and B is just a potential ligand ( $m = 1$ ), has been examined in detail elsewhere<sup>24,25</sup> and was implemented under the title of Two Sequential Binding Sites (TSBS) model in the Origin software designed to analyze binding isotherms from MicroCal ITC calorimeters.<sup>28</sup> Because three complex species with 1:1, 1:2, and 2:1 stoichiometries might coexist with the free monomers in CD + SDS aqueous solutions, specially when  $\gamma$ -CD is present,<sup>20</sup> we decided to develop our own software (available upon request from Á.P.) to analyze the calorimetric isotherms.

**Fitting Procedure.** The simulated annealing algorithm<sup>31</sup> was employed to minimize  $\chi^2$  (eq 5) as a function of the adjustable parameters  $K_{11}$ ,  $K_{12}$ ,  $K_{21}$ ,  $\Delta H_{11}^\circ$ ,  $\Delta H_{12}^\circ$ , and  $\Delta H_{21}^\circ$ .

$$\chi^2 = \frac{1}{p-v} \sum_{i=1}^p [Q_i(\text{exp}) - Q_i(\text{mod})]^2 \quad (5)$$

In the later expression,  $p$  and  $v$  stand for the number of experimental points and degrees of freedom, respectively. The employed fitting program, written in C code, was integrated in a series of Linux bash scripts to perform a minimum of 5000 independent minimizations for each isotherm. These include six-parameter

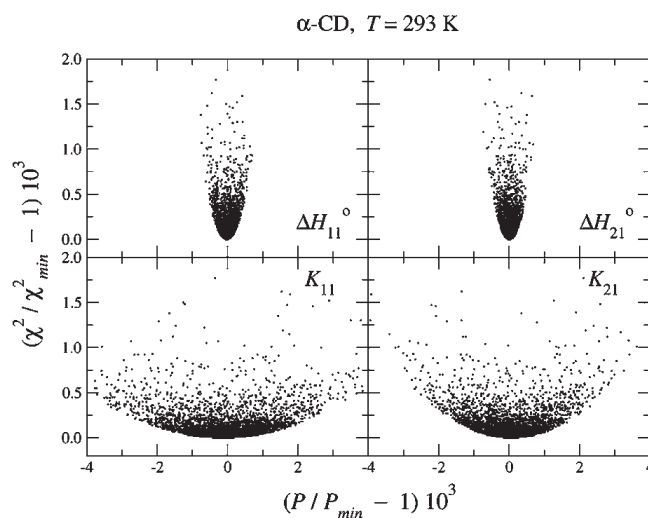


**Figure 1.** Projections of the  $\chi^2$  profile on the dimensions of  $\Delta H_{11}^\circ$ ,  $\Delta H_{21}^\circ$ ,  $K_{11}$ , and  $K_{21}$ , obtained from the fitting of the isotherm involving  $\alpha$ -CD at 293 K. For clarity, only the vicinity of the global minimum is shown. Each axis is normalized as indicated in the corresponding title, where  $P$  denotes any of the adjustable parameters and the subscript “min” refers to the global minimum. The axes are in the same scale in the four plots to facilitate the comparison.

minimizations with no restrictions and four-parameter minimizations in which the presence of either 1:2 or 2:1 species is assumed to be negligible so that  $(K_{12}, \Delta H_{12}^\circ)$  or  $(K_{21}, \Delta H_{21}^\circ)$  are zero. Each minimization starts from random seeds and involves about  $10^5$  evaluations of  $\chi^2$  using different parameter values. This allows access to some local minima, as well as the determination of the objective function profile in the geometric space defined by the fitting parameters. The whole fitting process took about 3 days of calculation time in a normal desktop Linux computer. The dispersion of the  $\chi^2$  profile projection on each parameter dimension was employed to calculate the corresponding uncertainty (representative examples of these plots for each cyclodextrin, normalized to facilitate the comparison between systems and different parameters, are supplied in Figures 1, S1, and S2). As in a previous work,<sup>30</sup> the concentration of the free species,  $[A_f]_j$  and  $[B_f]_j$ , for each parameter set was determined by using the Newton–Raphson algorithm, thus making the determination of the population of every species at any  $[A]_j/[B]_j$  ratio straightforward. All isotherms were also analyzed using the TSBS model implemented in the MicroCal software, assuming that either the 1:2 or the 2:1 species are not present in the solution. In most cases, the results obtained from our methodology and that of the commercial software were indistinguishable, the exceptions reaching lower  $\chi^2$  values with our program. This was not unexpected, as the simulated annealing algorithm is characterized by its high performance in finding the global minimum of any multiple-parameter function.<sup>31</sup> Notably, the uncertainties provided by Origin were significantly different from those estimated from the  $\chi^2$  profiles. As a way of example, the  $\chi^2$  profile projections shown in Figure 1 for  $\{\alpha\text{-CD} + \text{SDS}\}$  at 293 K point to higher relative uncertainties of  $(K_{11}, \Delta H_{11}^\circ)$  as compared to those of  $(K_{21}, \Delta H_{21}^\circ)$ . In this line, the relative uncertainties obtained with our program were (1.6, 0.2)% and (0.9, 0.1)%, respectively; by contrast, Origin provided (1.3, 0.3)% for each pair. Thus, all of the results presented and discussed in this Article are based on our codes.



### 3. BACKGROUND AND CONTEXT OF THE STUDY: A CRITICAL REVIEW

A thorough review of thermodynamic data for the CD:SDS complex formation has been performed (Tables 1 and 2),<sup>32–72</sup> paying special attention to the binding constants. It should be emphasized the lack of temperature-dependent surveys,<sup>55</sup> as well as the fact that almost all of the available quantities refer to the standard temperature 298 K. As illustrated by Table 3 (in section 4.1), the magnitude and even the sign of the thermodynamic parameters may vary with temperature, due to the large heat capacities usually involved in the CD-inclusion complex formation.<sup>73</sup> It is worth noting that the  $\beta$ -CD:SDS system is by far the most studied, in agreement with the fact that  $\beta$ -CD is the most generally used complexing agent in pharmaceutical chemistry.<sup>74</sup> Besides the works cited in Table 2, complementary thermodynamic studies have shown that the formation of  $\beta$ -CD:SDS complexes accounts for the particular behavior of dilution enthalpies, osmotic coefficients, and apparent molar volumes of SDS in {CD+SDS} aqueous solutions.<sup>75,76</sup>

#### 3.1. Overlooking Second-Order Species: A Common Issue.

Another remarkable feature in Tables 1 and 2 is that in about three-quarters of cases no data are provided for binding constants other than  $K_{11}$ , despite the existence of ternary species like  $\alpha$ -CD<sub>2</sub>SDS<sub>1</sub> and  $\beta$ -CD<sub>2</sub>SDS<sub>1</sub> being commonly accepted nowadays. As early as 1986, Hersey et al.<sup>35</sup> inferred from conductivity and reaction kinetics studies at 298 K that the dominant inclusion complex at concentration ratios  $[\alpha\text{-CD}]/[\text{SDS}] \geq 2$  contains two cyclodextrin molecules per SDS. This was later confirmed by ITC<sup>41</sup> and even by indirect methods like protein refolding assisted by  $\alpha$ -CD:SDS complexation.<sup>77</sup> As regards  $\beta$ -CD, Palepu and Reinsborough<sup>36</sup> (1988) were the first to conclude from conductance measurements in the SDS premicellar region that the amount of 2:1 complex is significant at concentration ratios  $[\beta\text{-CD}]/[\text{SDS}] \geq 1.1$  and 298 K, which was recently ascertained by <sup>1</sup>H NMR<sup>58</sup> and by phase behavior studies of mixed systems.<sup>78</sup> The average  $[\beta\text{-CD}]/[\text{SDS}]$  ratio in inclusion complexes was found to be smaller than 1.1 by capillary electrophoresis,<sup>69</sup>  $1.1 \pm 0.3$  by cyclic voltammetry,<sup>79</sup> about 1.2 from conductivity data,<sup>76</sup> and  $1.3 \pm 0.1$  from speed of sound measurements.<sup>52</sup> The differences in the mode of complexation between  $\alpha$ -CD and  $\beta$ -CD were explained by Tsianou and Alexandridis<sup>80</sup> on the basis of geometrical considerations, arguing that the smaller internal diameter of  $\alpha$ -CD favors a fully extended SDS chain (of 16 Å length<sup>81</sup>) that would easily thread two cyclodextrins (natural CDs are 7.9 Å high), while the wider cavity of the  $\beta$ -CD favors the appearance of kinks in the SDS chain, thus reducing the probability of 2:1 complex formation. SDS-dehydration comparative studies performed by MD simulations on  $\alpha$ -CD<sub>2</sub>SDS<sub>1</sub> and  $\beta$ -CD<sub>2</sub>SDS<sub>1</sub> complexes support such rationalization.<sup>20</sup> More generally, within any homologous series of hydrogenated surfactants differing in their tail length, the onset of the 2:1 complex formation appears to be lower for  $\alpha$ -CD than for  $\beta$ -CD, because the chain fraction included by  $\alpha$ -CD adopts an all-trans conformation while  $\beta$ -CD enables the surfactant chain to coil by adopting gauche conformations.<sup>82</sup> The absence of reported  $K_{ij}$  data ( $i, j = 1, 2; i \neq j$ ) in the literature regarding CD:SDS inclusion complexes is usually rationalized under the assumption that  $i:j$  species have a negligible presence or do not even exist. Such a premise is forced in many cases by the low sensitivity of the employed experimental technique. When  $K_{11}$  and  $K_{ij}$  are the same order of magnitude, such inconvenience can be overcome

by furnishing the overall binding constant  $\beta_{ij} = K_{11}K_{ij}$ , instead of trying to determine the stepwise binding constants separately (see Table 1).<sup>35,43,46,83</sup> Moreover, Pistolis and Malliaris<sup>84,85</sup> showed that differentiation between 1:1 and 2:1 stoichiometries by means of computer fitting methods or double-reciprocal plot techniques is not always possible, in which case it is imperative that direct methods be employed to determine the stoichiometry unambiguously. Yet the experimental (or methodological) sensitivity is not the only to blame: As pointed out by Wilson and Verrall,<sup>82</sup> it is also possible to overlook additional complexation equilibria when operating in a limited range of concentration ratios, particularly when  $K_{11}$  and  $K_{ij}$  vastly differ in magnitude. As a way of example, a recent comparison of the <sup>1</sup>H NMR spectra for SDS and its equimolar mixture with  $\alpha$ -CD did not allow the authors to infer the existence of  $\alpha$ -CD<sub>2</sub>SDS<sub>1</sub> complexes.<sup>86</sup>

#### 3.2. The Problem of Data Inconsistency and Its Sources.

Still, the most striking feature in Tables 1 and 2 is that the range of reported  $K_{11}$  values is so wide ( $[0.1, 66.6] \text{ mM}^{-1}$  and  $[0.21, 49] \text{ mM}^{-1}$  for  $\alpha$ -CD and  $\beta$ -CD complexes, respectively) that it provides little support for any subsequent new value; that is, the fact of a new value being within that range is hardly an accreditation.<sup>47,87</sup> Furthermore,  $K_{11}$  for  $\beta$ -CD:SDS was found to be strongly dependent on the SDS concentration (within the precmc region) by some authors,<sup>36,38,62</sup> against what might be expected from a proper thermodynamic standpoint. Such kind of inconsistency has also been described for CD-inclusion complexes involving other long hydrocarbon chain surfactants and has been interpreted as arising from a modification in the surfactant solution organization or/and from the presumption of 1:1 stoichiometry.<sup>38,62,88</sup> A similar finding as regards  $K_{21}$  (found to be dependent on both SDS and  $\beta$ -CD concentration) was partly ascribed by Park and Song<sup>62</sup> to self-association of 1:1 complexes. It is worth mentioning that their line of argument has been recently recovered by Loftsson et al.<sup>89</sup> within a more general frame (see below). The issue about the origin of the great discrepancy between the  $K_{11}$  values reported for a given system has been raised by many authors, but there is no general agreement at this respect. Some common causal agents that could be easily avoided are: (i) the above-mentioned presumption of 1:1 stoichiometry<sup>88,90</sup> (which takes importance when  $K_{11}$  and  $K_{ij}$  are the same order of magnitude, as in  $\alpha$ -CD:SDS and  $\gamma$ -CD:SDS complexes), (ii) the use of a model of identical and independent sites to describe systems that are known to be by far positively cooperative (for markedly negatively cooperative systems,<sup>24</sup> such model would consistently fit to a unique binding site, which is an acceptable approach), (iii) the confusion between intrinsic, stepwise, and overall binding constants (which are incomparable with each other unless the average stoichiometry of complexes is 1:1 within error, as explained in the Supporting Information), (iv) the unawareness about the high water content of CDs<sup>91</sup> (which is in the region of 10–15% and can not be entirely removed by drying nor by repeated recrystallization,<sup>92,93</sup> thus forcing to its accurate determination), and (v) the careless operation in the surfactant micellar region (for example, when data are treated by disregarding the competition between micellization and CD-complexation). This later factor is particularly relevant, given that a number of traditional methods for the determination of the binding constants are based on surveying the increase of the apparent cmc with the cyclodextrin concentration while assuming that CD becomes saturated before micellization. García-Río et al.<sup>54</sup> pointed out that such methods are useless due to the existence in the solution of a significant amount of uncomplexed CD. This issue

(recently reviewed by Xing et al.<sup>94</sup>) is a particular case of another frequent source of discrepancy, that the theoretical bases of some reliable experimental studies fail in interpreting the measurements in terms of equilibrium concentration of different species.<sup>66,90</sup>

**3.2.1. The Effect of Noninclusion Complexes and Aggregation Phenomena.** In line with the latter statement, we do not want to leave unmentioned a potential (and almost unavoidable) source of noise in the case of experiments involving  $\beta$ -CD: the CD-induced aggregation of SDS below its cmc. Direct evidence for this effect was first provided by Jiang and Wang,<sup>95</sup> and subsequently confirmed by others.<sup>96,97</sup> The former pointed to the  $\beta$ -CD:SDS inclusion complex as the hydrophobic source inducing the aggregation. According to the different reports, the critical aggregate concentration for SDS in the presence of  $\beta$ -CD would be located within the range 0.8–6 mM, whose broadness reveals the need of making a more in-depth investigation of that phenomenon. Actually, this appears to be just a particular case of a more general issue that was recently reviewed by Loftsson et al.,<sup>89</sup> the coexistence of various complex structures in solution caused by the (partly concentration dependent) self-aggregation of cyclodextrins and cyclodextrin complexes and by the presence of noninclusion complexes. As stated by Loftsson and coauthors, this fact could explain why the experimentally determined values of  $K_{11}$  for CD-based inclusion complexes are highly sensitive to both the method applied and the composition of the medium, because they would actually be apparent binding constants describing the combining effect of the various coexisting complex structures. Specifically, stable noninclusion complexes such as SDS/ $\beta$ -CD<sub>1</sub>SDS<sub>1</sub> and SDS/ $\beta$ -CD were observed by MD simulations in a previous work,<sup>20</sup> where we hypothesized that those arrays could act as a sort of nucleation points for the reported ( $\beta$ -CD)-induced aggregation of SDS below its cmc. Attempts to determine the (small) binding constant characterizing a CD-based noninclusion complex have been scarce.<sup>98</sup>

**3.2.2. Some Notes on the Solvent Influence and the Technique Sensitivity.** There are other technique-related factors limiting the reliability of the resultant binding constants. For instance, the affinities (as defined by  $-\Delta G^\circ$ ) are known to be somewhat influenced by the ionic strength of the medium,<sup>47,73</sup> which varies upon the addition of a pH buffer, not to mention that certain ionic solutes become unstable with pH changes,<sup>51</sup> or that CD deprotonation can be induced if the solution becomes too alkaline.<sup>54</sup> Another paradigmatic case of solvent influence is the solvent isotope effect associated with the use of D<sub>2</sub>O, whose dipole moment is higher than that of H<sub>2</sub>O (1.8547 D against 1.8527 D).<sup>99</sup> It has been shown that host–guest equilibrium constants increase significantly (in the order of 10–50%) when changing from H<sub>2</sub>O to D<sub>2</sub>O.<sup>100</sup> Therefore, affinities coming from <sup>1</sup>H NMR spectroscopy should be regarded with some caution. Moreover, certain techniques were signaled not to allow accurate determination of very high binding constants,<sup>41</sup> while others were reported to be inappropriate for estimating very low affinities.<sup>47</sup> This is the case of the phenolphthalein competition method, whose application led just to the determination of  $K_{11}$  in the six examples displayed in Tables 1 and 2 for  $\gamma$ -CD and  $\beta$ -CD complexes, while the use of the same principle with a fluorescent probe gave both  $K_{11}$  and  $K_{21}$  in the three cases illustrated in Table 2. Furthermore, according to Funasaki et al.,<sup>101</sup> there are a number of techniques that are not very suitable for the estimation of  $K_{ij}$  when  $K_{ij} \ll K_{11}$ , because the observed quantities exhibit monotonic changes with increasing concentration of the surfactant and cyclodextrin. In other instances, the sensitivity of the

selected technique is so low that it even fails to ensure consistent  $K_{11}$  values: an example is the widely used conductometric method (when dealing with ionic surfactants), which lies on the (small) difference in electric conductivity between the associated and unassociated surfactant ions.<sup>62</sup>

**3.3. Addressing the Consistency Problem by a Two-Class Categorization of the Experimental Techniques.** The problem concerning the consistency of experimentally determined ligand-macromolecule binding constants was addressed in 1995 by Mwakibete et al., prompted by the wide spread exhibited by  $K_{11}$  values at 298 K for  $\beta$ -CD:SDS complexes.<sup>19</sup> They noticed that the set of available experimental techniques can be subdivided into two categories, which we have labeled as I and II. Methods from group I take advantage of the existence of any physically observable properties that are proportional in some way to the extent of binding, while those from group II rely on direct measurements of the free and bound ligand in a solution containing a known amount of the macromolecule. The authors concluded that only the techniques from group II appear to give consistent  $K_{11}$  (the corresponding  $K_{ij}$  being just qualitative estimates, especially if  $K_{ij} \ll K_{11}$ ). They also pointed out that the isothermal titration calorimetry is an exception to this rule, because it is a technique that has been specifically designed to measure binding isotherms and subsequently obtain complexation constants. Hence, although ITC would belong to group I, it might be included in group II from a practical standpoint. Tables 1 and 2 display chronologically organized data for every system and category following Mwakibete criterion, with the aim of assessing its current applicability under the light of the above discussion on discrepancy sources.

**$\alpha$ -Cyclodextrin.**  $K_{11}$  data from groups I and II clearly differ by 1–2 orders of magnitude. However, the  $\beta_{21}$  obtained from reaction kinetics (group I) by Hersey et al.<sup>35</sup> (490 mM<sup>−2</sup>) compares relatively well with our  $K_{11}K_{21}$  product (446 mM<sup>−2</sup>). Among data from group II (other than ours), only those from Wan Yunus et al.<sup>40</sup> are consistent with the later values ( $K_{11}K_{21}$  amounts to 378 mM<sup>−2</sup>). The remainder data sources in group II are associated with some inadvisable practices, like the operation in the postcmc range by overlooking the coexistence of several equilibria,<sup>43</sup> the employ of a rather restricted range of concentration ratios,<sup>44</sup> or the application of a Single Set of Identical Sites model in a context of positive cooperativity<sup>42</sup> (see footnotes in Table 1 for more details).

**$\beta$ -Cyclodextrin.** First, it should be noted that the expansion and update of the  $\beta$ -CD:SDS  $K$  database handled by Mwakibete et al.<sup>19</sup> (which was composed of 9 elements, against the current 39 displayed in Table 2) is expected to give more insight on the validity of their proposal. It was pointed out<sup>38</sup> that a  $K_{11}$  value below 3 mM<sup>−1</sup> (9 out of 10 are found in group I) is not consistent with the values reported for the complexes between  $\beta$ -CD and other surfactants with a C<sub>12</sub> hydrocarbon chain. In average,  $K_{11}$  data from group II are 1 order of magnitude higher than those coming from group I, but such differentiation is not that neat when a point-by-point inspection is performed. Thus, the  $K_{11}$  values reported by García-Río et al.<sup>57</sup> from reaction kinetics and by Jiang et al.<sup>60</sup> from <sup>1</sup>H NMR spectroscopy (both of them in group I) are comparable to ours (23.0 and 24.5 mM<sup>−1</sup>, respectively, against 20.8 mM<sup>−1</sup>). It is interesting to note that García-Río had previously<sup>54</sup> obtained  $K_{11} = 8.0$  mM<sup>−1</sup> with the same technique but at alkaline conditions (where  $\beta$ -CD is deprotonated). This sharp drop of the binding constant with a pH increase is caused by the electrostatic repulsion between

Table 1. Review of Thermodynamic Data for the Formation of  $\alpha$ -CD:SDS and  $\gamma$ -CD:SDS Complexes at 298 K<sup>a,b,c</sup>

$10^{-3}K_{11}$ (M <sup>-1</sup> )	$10^{-3}K_{ij}$ (M <sup>-1</sup> )	$10^{-6}\beta_{ij}$ (M <sup>-2</sup> )	technique	source
<b><math>\alpha</math>-CD:SDS Complexes</b>				
group I techniques <sup>d</sup>				
0.111 ± 0.006 <sup>e</sup>			static conductivity	Okubo et al., 1976 <sup>32</sup>
1.41 ± 0.52 <sup>e</sup>			reaction kinetics <sup>f</sup>	Kitano and Okubo, 1977 <sup>33</sup>
1.12 <sup>e</sup>			static conductivity	Satake et al., 1985 <sup>34</sup>
		490 <sup>g</sup>	reaction kinetics <sup>f</sup>	Hersey et al., 1986 <sup>35</sup>
0.754 <sup>e</sup>			static conductivity	Palepu and Reinsborough, 1988 <sup>36</sup>
0.10 <sup>e</sup>			dynamic conductivity <sup>h</sup>	Okubo et al., 1989 <sup>37</sup>
0.16 <sup>e,i</sup>				
2.48 <sup>e</sup>			static conductivity	Aman and Serve, 1990 <sup>38</sup>
0.142 ± 0.008 <sup>e</sup>			static conductivity	Sehgal et al., 2006 <sup>39</sup>
group II techniques <sup>d</sup>				
21	18		emf <sup>j</sup>	Wan Yunus et al., 1992 <sup>40</sup>
			ITC <sup>k,l</sup>	Turco Liveri et al., 1992 <sup>41</sup>
66.6 ± 3.4 <sup>m</sup>	16.65 ± 0.85 <sup>m</sup>		ITC <sup>n</sup>	Ikeda et al., 2000 <sup>42</sup>
		0.113 <sup>o</sup>	ITC <sup>p,q</sup>	Liao et al., 2009 <sup>43</sup>
0.126 <sup>e,r</sup>			spectral displacement <sup>s,t</sup>	Al-Sherbini, 2009 <sup>44</sup>
19.3 <sup>e</sup>			ITC <sup>u</sup>	Liu et al., 2010 <sup>45</sup>
28.2 ± 0.3	15.8 ± 0.2		ITC <sup>u</sup>	this work
<b><math>\gamma</math>-CD:SDS Complexes</b>				
group I techniques <sup>d</sup>				
0.83 <sup>e</sup>			static conductivity	Palepu and Reinsborough, 1988 <sup>36</sup>
		0.01700 ± 0.00026	static conductivity	Sehgal et al., 2008a <sup>46</sup>
group II techniques <sup>d</sup>				
0.940 <sup>e,v</sup>			ITC <sup>k,w</sup>	Turco Liveri et al., 1992 <sup>41</sup>
0.69 ± 0.05 <sup>e</sup>			spectral displacement <sup>s,x</sup>	Gray et al., 1995 <sup>47</sup>
2.181 ± 0.008	0.78 ± 0.06		ITC <sup>u</sup>	this work

<sup>a</sup>Data were not found at other temperatures. <sup>b</sup>The subscripts  $ij$  stand for  $\alpha$ -CD<sub>2</sub>SDS<sub>1</sub> and  $\gamma$ -CD<sub>1</sub>SDS<sub>2</sub> species, respectively. <sup>c</sup> $\beta_{ij} = K_{11}K_{ij}$ . <sup>d</sup>As suggested by Mwakibete et al. (ref 19). <sup>e</sup> $\alpha$ -CD<sub>2</sub>SDS<sub>1</sub> (or  $\gamma$ -CD<sub>1</sub>SDS<sub>2</sub>) complex formation is a priori assumed either not to take place or to be negligible. <sup>f</sup>Absorbance measured with a stopped-flow spectrophotometer. <sup>g</sup> $\Delta H_{21}^\circ$  (overall) = -38 kJ/mol, calculated by evaluating  $\beta_{21}$  at several temperatures (data not provided). <sup>h</sup>Stopped-flow method; two different models are applied. <sup>i</sup> $\Delta H_{11}^\circ$  = (-7 ± 2) kJ/mol,  $T\Delta S_{11}^\circ$  = (5 ± 1) kJ/mol. <sup>j</sup>Electromotive force study using ion (SDS) selective electrodes. <sup>k</sup>TAM 2277-204 model, from LKB. <sup>l</sup>No binding constant is provided; the authors only report the standard enthalpy associated with the direct formation of the  $\alpha$ -CD<sub>2</sub>SDS<sub>1</sub> complex from the free  $\alpha$ -CD and SDS,  $\Delta H_{21}^\circ$  (overall) = (-32.0 ± 0.5) kJ/mol. <sup>m</sup>By fitting the experimental data to a Single Set of Identical Sites (SSIS) model for CD<sub>n</sub>SDS<sub>1</sub> complexes, the existence of two binding sites was reported ( $n = 1.92 \pm 0.02$ ) with an intrinsic binding site constant  $K = 33.3 \pm 1.7$  (from which the stepwise binding constants can be derived as  $K_{11} = 2K$  and  $K_{21} = K/2$ ). Contributions to the intrinsic binding energy:  $\Delta H^\circ = -35.2$  kJ/mol, and  $T\Delta S^\circ = -9.4$  kJ/mol. <sup>n</sup>Omega model, from MicroCal. <sup>o</sup>The authors also report  $\Delta H_{21}^\circ$  (overall) = -32 kJ/mol and  $T\Delta S_{21}^\circ$  (overall) = -11 kJ/mol, but the standard Gibbs energy change  $\Delta G_{21}^\circ$  (overall) calculated from these quantities (-21 kJ/mol) disagrees with that calculated from the overall binding constant  $\beta_{21}$  (-28.8 kJ/mol). <sup>p</sup>The original MicroCal-ITC model, as described by Wiseman et al. (ref 21). <sup>q</sup>Titrations of 200 mM SDS were performed, until a final SDS concentration of about 4.5 times the cmc was attained in the measuring cell. <sup>r</sup>Value obtained from qualitative estimations based on the comparison of the spectral behavior at two different  $[\alpha\text{-CD}]/[\text{SDS}]$  ratios. <sup>s</sup>Indirect absorbance method: competitive binding study using a probe. <sup>t</sup>UV-visible probe: 0.03 mM solution of a merocyanine dye. Absorbance changes obtained at 406 nm. <sup>u</sup>VP-ITC model, from MicroCal. <sup>v</sup>Value given in molality scale (meaning that the standard state is not 1 M as usual, but 1 m);  $\Delta H_{11}^\circ$  = (-28.3 ± 0.5) kJ/mol. The authors explore the possibility of 2:1 complexation, concluding that only 1:1 species are present. <sup>w</sup>Calorimetric measurements were mainly performed at SDS concentrations greater than its cmc. <sup>x</sup>Visible probe: 0.02 mM phenolphthalein. Solutions buffered at pH 10.2 with 0.05 M NaHCO<sub>3</sub>/0.10 M NaOH solution. Absorbance changes obtained at 552 nm.

the  $\beta$ -CD anion and SDS and has been documented for other anionic surfactants too.<sup>102</sup> In group II, both the electromotive force study from Wan Yunus et al.<sup>40</sup> and the spectral displacement method using diverse fluorescent probes<sup>62,66,71</sup> furnish  $K_{11}$  and  $K_{21}$  consistent with the values reported here. More specifically, among them we deem the  $K_{11}$  provided by Park and Song<sup>62</sup> (25.6 mM<sup>-1</sup>) to be a good reference because the CD concentrations appear to be corrected for water content only in their work. From our general experience with CD-based complexes, disregarding the CD water content affects dramatically the relative values of the stepwise binding constants and even their order of

magnitude (see last footnote in Table 3). As regards  $K_{21}$ , Wintgens and Amiel<sup>71</sup> claimed that their value (0.64 mM<sup>-1</sup>) is more accurate than that reported by Park and Song, as they used a more refined model to consider a species that is usually ignored for the sake of simplicity (the probe/ $\beta$ -CD complex). It is reassuring to remark that our  $K_{21}$  (0.77 mM<sup>-1</sup>) is in good agreement with them.

**$\gamma$ -Cyclodextrin.** The small amount of available data (Table 1) does not allow one to extract conclusions in this case. The pair ( $K_{11}$ ,  $K_{12}$ ) is furnished for the first time in the present work. Previous approaches had neglected the formation of 1:2 species,



with the exception of a conductometric study<sup>46</sup> (group I) that provided a  $\beta_{12}$  value inconsistent with ours ( $0.02 \text{ mM}^{-2}$  against  $1.7 \text{ mM}^{-2}$ ).

From the above analysis, it can be concluded that the employ of a technique from group II does not guarantee data consistency: Failings of the experimental procedure, the employ of unjustified assumptions, the application of an oversimplified model, and the insufficient sensitivity of the instrumentation or of the method are recurrent factors leading to inconsistent binding constants within that group. Vice versa, it is possible to overcome the disadvantages inherent to techniques from group I so as to obtain at least reliable  $K_{11}$  or  $\beta_{ij}$  data, provided that common discrepancy-causal agents are avoided, the method is well designed, the instrumentation is sensitive enough, and a theoretically sound model is used. Therefore, the Mwakibete-assumed exceptionality of the ITC is not anything of the sort (in fact, Tables 1 and 2 show a manifest disagreement between the ITC results from different sources). The examination of Tables 1 and 2 has just disclosed the potential of the reaction kinetics<sup>35,57</sup> and the  $^1\text{H}$  NMR spectroscopy,<sup>60</sup> but the surface tension already proved its ability to bring accurate  $K_{11}$ ,  $K_{21}$ , and  $K_{12}$  simultaneously, also in the context of CD-based inclusion complexes.<sup>30</sup>

#### 4. RESULTS AND DISCUSSION

The thermodynamic quantities shown in Table 3 reflect a delicate balance between several contributions whose concerted interplay is necessary to achieve recognition between the host and guest molecules. In the literature, there is a general agreement in that the main contributions to the formation of CD inclusion complexes are:<sup>73</sup> (i) dehydration of the guest molecule that is inserted into the CD cavity; (ii) interaction of the guest molecule with the interior of the CD; (iii) expulsion of water molecules from the CD cavity; (iv) CD-guest hydrogen-bonding interactions; (v) changes in the surrounding water network of the CD; and (vi) conformational changes of the CD and SDS upon complexation. These contributions are expressed in terms of

molecular level events that are outside the scope of thermodynamics. However, molecular dynamics simulations are particularly well suited to (a) confirm or disregard the existence of a given contribution, (b) evaluate the frequency of occurrence of a given molecular level event, and (c) provide a qualitative assessment of the interactions that determine the formation and the stability of the inclusion complexes. Earlier MD simulations<sup>20</sup> have been analyzed in terms of contributions (i)–(vi) for the same inclusion complexes studied here. Table 4 summarizes the most relevant microscopic data from those MD simulations for contributions (i), (iii), (iv), and (v). The quantification of molecular events displayed in Table 4 is the basis for the evaluation of the corresponding individual contributions to the thermodynamics quantities.

**4.1. Thermodynamics of the Complex Formation Processes.** ITC experiments for  $\alpha$ -,  $\beta$ -, and  $\gamma$ -cyclodextrin+SDS in water were performed at several temperatures between 283 and 323 K. The experimental data are displayed in the form of integrated heat change per injection (or stepwise heat change) normalized for moles of injectant against the molar ratio of solutes (Figures 2–4). For clarity, the results are presented separately for each CD.

*$\alpha$ -Cyclodextrin.* The set of binding isotherms at six temperatures between 283 and 308 K is shown in Figure 2. The titration equivalence point (inflection point) of each isotherm is located at a molar ratio  $[\text{SDS}]/[\alpha\text{-CD}]$  of approximately 0.5, pointing to the existence of  $\alpha\text{-CD}_2\text{SDS}_1$  complexes regardless of the temperature. When the SBS model was applied by considering the simultaneous presence of  $\alpha\text{-CD}_1\text{SDS}_1$ ,  $\alpha\text{-CD}_2\text{SDS}_1$ , and  $\alpha\text{-CD}_1\text{-SDS}_2$  complexes, either it afforded  $K_{12} = 0$  within error or the global minimum of the objective function did not decrease significantly with respect to the four-parameter fitting accounting for 1:1 and 2:1 species alone. Moreover, the alternative four-parameter fitting ignoring the presence of 2:1 complexes provided  $\chi^2$  values that were 3 orders of magnitude higher. Hence, the 1:1/2:1 option was taken as the satisfactory fit in all instances (see fitted curves in Figure 2 and parameters in Table 3), agreeing

**Table 2. Review of Thermodynamic Data for the  $\beta$ -CD:SDS Complex Formation at 298 K<sup>a</sup>**

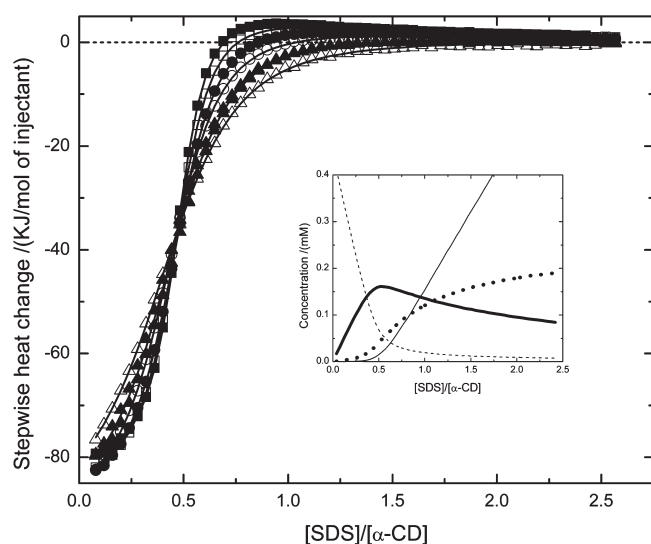
$10^{-3}K_{11} \text{ (M}^{-1}\text{)}$	$10^{-3}K_{21} \text{ (M}^{-1}\text{)}$	$10^{-3}K_{12} \text{ (M}^{-1}\text{)}$	technique	source
group I techniques <sup>b</sup>				
$0.356 \pm 0.018^c$			static conductivity	Okubo et al., 1976 <sup>32</sup>
$4.55 \pm 0.83^c$			reaction kinetics <sup>d</sup>	Kitano and Okubo, 1977 <sup>33</sup>
$3.63^c$			static conductivity	Satake et al., 1986 <sup>48</sup>
$0.300^c$			static conductivity	Georges and Desmetre, 1987 <sup>49</sup>
$1.38\text{--}7.23^{c,e}$			static conductivity	Palepu and Reinsborough, 1988 <sup>36</sup>
$3.2\text{--}17.5^{c,e}$			static conductivity	Aman and Serve, 1990 <sup>38</sup>
$5.0 \pm 0.8^c$			static conductivity <sup>f</sup>	Funasaki et al., 1992 <sup>50</sup>
$5.5 \pm 1.9^g$				
$5.4 \pm 1.0^h$				
$0.210 \pm 0.018^c$				
$1.21 \pm 0.13^c$				
$0.733 \pm 0.080^i$				
$3.6 \pm 1.0^j$				
$8.4 \pm 1.2^k$				
$1.0 \pm 0.2^l$	$0.25 \pm 0.05^l$		surface tension	Dharmawardana et al., 1993 <sup>51</sup>
$4.32 \pm 0.67^c$			speed of sound	Junquera et al., 1993 <sup>52</sup>
$8.0 \pm 0.5^{c,n}$			$^1\text{H}$ NMR spectroscopy <sup>m</sup>	Guo et al., 1994 <sup>53</sup>
			reaction kinetics <sup>o</sup>	García-Río et al., 1997 <sup>54</sup>
			surface tension <sup>p</sup>	Yin et al., 2001 <sup>55</sup>

Table 2. Continued

$10^{-3}K_{11}$ ( $M^{-1}$ )	$10^{-3}K_{21}$ ( $M^{-1}$ )	$10^{-3}K_{12}$ ( $M^{-1}$ )	technique	source
$0.453 \pm 0.006^a$			surface tension	Bo et al., 2006 <sup>56</sup>
$23.0 \pm 0.5^c$			reaction kinetics <sup>o</sup>	García-Río et al., 2007 <sup>57</sup>
$49 \pm 26^g$			$^1H$ NMR spectroscopy <sup>m</sup>	Xing et al., 2007 <sup>58</sup>
$0.294 \pm 0.013^c$			static conductivity	Sehgal et al., 2008b <sup>59</sup>
$24.5^c$			$^1H$ NMR spectroscopy <sup>m</sup>	Jiang et al., 2009 <sup>60</sup>
$3.021 \pm 0.098^c$			capillary electrophoresis <sup>r</sup>	Bendazzoli et al., 2010 <sup>61</sup>
group II techniques <sup>b</sup>				
25.6	$0.22 \pm 0.09$		spectral displacement <sup>s,f</sup>	Park and Song, 1989 <sup>62</sup>
$19 \pm 1^c$			spectral displacement <sup>s,u</sup>	Sasaki et al., 1989 <sup>63</sup>
$18.5 \pm 0.3^c$			spectral displacement <sup>s,v</sup>	Sasaki et al., 1990 <sup>64</sup>
21	0.21		emf <sup>w</sup>	Wan Yunus et al., 1992 <sup>40</sup>
			ITC <sup>x,y</sup>	Turco Liveri et al., 1992 <sup>41</sup>
$9.6 \pm 0.5^c$			spectral displacement <sup>s,z</sup>	Gray et al., 1995 <sup>47</sup>
$15 \pm 2^{c,\alpha}$			spectral displacement <sup>s,\beta</sup>	Wilson et al., 1997 <sup>65</sup>
$26.8 \pm 2.5^z$	$0.44 \pm 0.09^z$		spectral displacement <sup>s,\delta</sup>	Shen et al., 1997 <sup>66</sup>
$1.55^e$		$0.795^e$	ITC <sup>e</sup>	Zhu et al., 1998 <sup>67</sup>
$8.15 \pm 0.40^{\phi}$			ITC <sup>\gamma</sup>	Eli et al., 1999 <sup>68</sup>
$48^{\eta}$	$0.21^{\eta}$		capillary electrophoresis <sup>\rho</sup>	Lin et al., 2001 <sup>69</sup>
$18.0 \pm 5.0^{z,\lambda}$			spectral displacement <sup>s,\mu</sup>	Guernelli et al., 2003 <sup>70</sup>
$18.2 \pm 0.4^{\tau}$	$0.64^{\tau}$		spectral displacement <sup>s,\theta</sup>	Wintgens and Amiel, 2004 <sup>71</sup>
$6.3^{\rho}$			ITC <sup>\sigma,\tau</sup>	Liao et al., 2009 <sup>43</sup>
$23.0 \pm 0.8^c$			ITC <sup>\omega</sup>	Jiang et al., 2010b <sup>72</sup>
$6.95^c$			ITC <sup>\psi</sup>	Liu et al., 2010 <sup>45</sup>
$20.8 \pm 0.1$	$0.77 \pm 0.03$		ITC <sup>\psi</sup>	this work

<sup>a</sup> Unless otherwise indicated. <sup>b</sup> As suggested by Mwakibete et al. (ref 19). <sup>c</sup> 2:1 complexation is a priori assumed either not to take place or to be negligible. <sup>d</sup> Absorbance measured with a stopped-flow spectrophotometer. <sup>e</sup>  $K_{11}$  appears to be SDS-concentration dependent, the lowest and the highest stated values corresponding to SDS 5 and 1 mM, respectively. <sup>f</sup> Three conductance-based models and four cmc-based models are applied to experimental conductance data taken from Palepu and Reinsborough (ref 36). <sup>g</sup> The model provides for 2:1 species, but affords a  $K_{21}$  value with an uncertainty of 100%. <sup>h</sup> The model provides for 1:2 species, but affords a  $K_{12}$  value with an uncertainty of 600%. <sup>i</sup> The model provides for 2:1 species, but affords a negative  $K_{21}$ . <sup>j</sup> The model provides for 1:2 species, but affords a negative  $K_{12}$ . <sup>k</sup> In the original work, the stated value for  $K_{11}$  is  $8.36 \pm 1.20$ ; we have rounded it off to express the uncertainty with no more than two significant digits. The model provides for the existence of 2:1 species, giving  $K_{21} = 0$  within error. <sup>l</sup> It was found that experimental data are consistent with a complex average stoichiometry of 1.3:1. The authors made use of this result to get the intrinsic binding site constant  $K = 0.5 \pm 0.1$  (from which the stepwise binding constants can be derived as  $K_{11} = 2K$  and  $K_{21} = K/2$  within the frame of a SSIS model). <sup>m</sup> In  $D_2O$ . <sup>n</sup> All CDs are assumed to be deprotonated under the alkaline conditions used,  $[NaOH] = 0.17$  M; hence  $K_{11}$  applies to the  $\beta$ -CD anion. <sup>o</sup> Absorbance measured with a spectrophotometer. <sup>p</sup> From the English abstract of ref 55, whose text is in Chinese, it can just be inferred that the employed model provides for stoichiometries other than 1:1. Besides, it is stated that "Some thermodynamic parameters of the binding process were calculated according to van't Hoff equation", which could imply that a temperature-dependent study was performed. <sup>q</sup> By fitting the experimental data to a SSIS model for  $CD_1SDS_n$  complexes, only one binding site was found ( $n = 1.07 \pm 0.03$ ); hence  $K = K_{11}$ . <sup>r</sup> New capillary electrophoresis approach based on electric current measurement (hence fitting in group I techniques). <sup>s</sup> Indirect absorbance method: competitive binding study using a probe. <sup>t</sup> Fluorescent probes: two anilidonaphthalenesulfonates. Excitation wavelengths: 320 and 350 nm; fluorescence emission at 460 and 500 nm, respectively. <sup>u</sup> Visible probe: 0.03 mM phenolphthalein in aqueous 4 mM  $Na_2CO_3$ . Absorbance changes obtained at 550 nm. <sup>v</sup> Visible probe: 0.03 mM phenolphthalein. Solutions buffered at  $pH \approx 10.5$  with  $Na_2CO_3$ . Absorbance changes obtained at 550 nm. <sup>w</sup> Electromotive force study using ion (SDS) selective electrodes. <sup>x</sup> TAM 2277-204 model, from LKB. <sup>y</sup> No binding constant is provided, the authors only report  $\Delta H_{11}^\circ = (-12.8 \pm 0.5)$  kJ/mol. <sup>z</sup> Visible probe: 0.02 mM phenolphthalein. Solutions buffered at  $pH$  10.2 with 0.05 M  $NaHCO_3$ /0.10 M NaOH solution. Absorbance changes obtained at 552 nm. <sup>\alpha</sup>  $T = 295$  K. <sup>\beta</sup> Visible probe: 0.02 mM phenolphthalein. Solutions buffered at  $pH = 10.5$  with 0.1 M  $Na_2CO_3$ . Absorbance changes obtained at 550 nm. <sup>\gamma</sup> Room temperature (not specified). <sup>\delta</sup> Fluorescent probe: 1  $\mu M$  solution of a substituted 3H-indole. Absorption band, 377–380 nm; fluorescence band, 483–493 nm. Solutions buffered at  $pH = 9.5$  with NaOH. <sup>\epsilon</sup> From the English abstract of ref 67, whose text is in Chinese. <sup>\phi</sup> By fitting the experimental data to a SSIS model for  $CD_nSDS_1$  complexes only one binding site was found (the  $n$  uncertainty being 0.03), from which  $K = K_{11}$ . Besides,  $\Delta H_{11}^\circ = -10.9$  kJ/mol and  $T\Delta S_{11}^\circ = 11.4$  kJ/mol. <sup>\gamma</sup> 4200-ITC model, from CSC. <sup>\eta</sup> The authors estimate that 2:1 species may exist by less than 10%.  $K_{21}$  is taken from Wan Yunus et al. (ref 40), and  $K_{11}$  is obtained by manual adjustment. It is stated that any  $K_{11}$  value in the range 21–48 fits well, the highest end affording the best fitting. <sup>\theta</sup> 20% (v/v) methanolic aqueous solution,  $pH = 7.0$ . Detection wavelength set at 215 nm. <sup>\lambda</sup> The model can provide for 2:1 species, but does not fit well under this assumption. It was found by electrospray ionization mass spectrometry that the complex average stoichiometry in the gas phase is 1.03:1. <sup>\mu</sup> Visible probe: 0.02 mM phenolphthalein. Solutions buffered at  $pH = 10.6$  with 0.1 M  $Na_2CO_3$ . Absorbance changes obtained at 550 nm. <sup>\tau</sup>  $T = 296$  K. Average value using three different fluorescent probes. <sup>\theta</sup> Fluorescent probes. Excitation wavelengths, 362–365 nm; fluorescence emission, 467–475 nm. <sup>\rho</sup> By fitting the experimental data to a SSIS model for  $CD_nSDS_1$  complexes, only one binding site was found, from which  $K = K_{11}$ . Besides,  $\Delta H_{11}^\circ = -22$  kJ/mol,  $T\Delta S_{11}^\circ = -1$  kJ/mol. <sup>\sigma</sup> The original MicroCal-ITC model, as described by Wiseman et al. (ref 21). <sup>\tau</sup> Titrations of 200 mM SDS were performed, until a final SDS concentration of about 4.5 times the cmc was attained in the measuring cell. <sup>\omega</sup> TAM 2277-201 model, from Thermometric AB. <sup>\psi</sup> VP-ITC model, from MicroCal.





**Figure 2.** Integrated heat change per mole of injectant versus  $[\text{SDS}]/[\alpha\text{-CD}]$  molar ratio at 283 (■), 288 (□), 293 (●), 298 (○), 303 (▲), and 308 K (△). Inset: Concentration of free  $\alpha\text{-CD}$  (dashed thin line), free SDS (solid thin line),  $\alpha\text{-CD}_1\text{SDS}_1$  complexes (dotted thick line), and  $\alpha\text{-CD}_2\text{SDS}_1$  complexes (solid thick line) as a function of the  $[\text{SDS}]/[\alpha\text{-CD}]$  ratio, calculated from the isotherm at 283 K.

with the overall picture provided by MD simulations at several temperatures (Table 4).<sup>20</sup> All isotherms display positive cooperativity ( $K_{11} < 4K_{21}$ ),<sup>24</sup> which becomes less marked as  $T$  increases. Thus, the Hill slope at half saturation,<sup>29</sup> calculated as  $2/[1 + (K_{11}/4K_{21})^{0.5}]$ , decreases from 1.4 at 283 K to nearly 1 at 308 K. Moreover, the relative uncertainty of  $K_{21}$  is lower than that of  $K_{11}$  in the range [283, 293] K (as is exemplified in Figure 1), which is additional evidence of the prevalent role of the  $\alpha\text{-CD}_2\text{SDS}_1$  complexes at low temperatures.<sup>4,18</sup> Both binding processes (1:1 and 2:1 complex formation) are enthalpy-driven. Only at 283 K is the formation of 1:1 species governed by both entropy and enthalpy. According to Brown,<sup>103</sup> “enthalpy-driven positive cooperativity occurs when binding of the first ligand results in a conformational change at the second binding site, rendering it higher affinity to the ligand.” In the present context, because the SDS-head is unlikely to be included into the  $\alpha\text{-CD}$  cavity,<sup>20</sup> such interpretation would imply that the protruding SDS chain in the 1:1 complex is more feasible to get threaded by the second CD than in the free state. This is more than reasonable if we consider that (1) in the free state the SDS-tail tends to be curled to minimize the solvent-exposed area, and (2) the small diameter of the  $\alpha\text{-CD}$  cavity does not allow the appearance of kinks in the hosted chain fraction, so that the protruding part cannot curl and partially hide inside the CD.<sup>20</sup> This feature is revealed in Table 4 by the comparison of the SDS-tail hydration in  $\alpha\text{-CD}_1\text{SDS}_1$  and  $\beta\text{-CD}_1\text{SDS}_1$  complexes, which is larger in the first case despite the absence of water molecules inside the  $\alpha\text{-CD}$  cavity. In the range [283, 298] K, the binding isotherms show a small and flat endothermic maximum that decreases in magnitude and moves toward increasing molar ratio  $[\text{SDS}]/[\alpha\text{-CD}]$  as the temperature increases (the maximum goes from  $\sim 0.94$  at 283 K to  $\sim 1.4$  at 298 K). Such maxima arise from the competition between 2:1 and 1:1 complexation equilibria in a context of positive cooperativity, with  $\Delta H^\circ_{21} < \Delta H^\circ_{11} < 0$  for the complex formation processes. During the titration of SDS in the calorimetric cell, the competition becomes evident in a certain range of

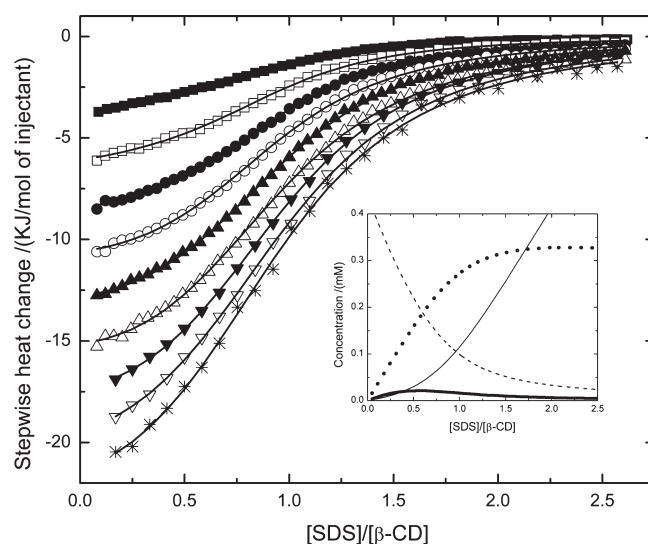


**Figure 3.** Integrated heat change per mole of injectant versus  $[\text{SDS}]/[\beta\text{-CD}]$  molar ratio at 283 (■), 288 (□), 293 (●), 298 (○), 303 (▲), 308 (△), 313 (▼), 318 (▽), and 323 K (\*). Inset: Concentration of free  $\beta\text{-CD}$  (dashed thin line), free SDS (solid thin line),  $\beta\text{-CD}_1\text{SDS}_1$  complexes (dotted thick line), and  $\beta\text{-CD}_2\text{SDS}_1$  complexes (solid thick line) as a function of the  $[\text{SDS}]/[\beta\text{-CD}]$  ratio, calculated from the isotherm at 283 K.

concentration ratios where the endothermic contribution coming from the rupture of previously formed 2:1 species surpasses the exothermic one from the formation of new 1:1 complexes. At 283 K, the maximum  $[\alpha\text{-CD}_2\text{SDS}_1]$  is reached at a molar ratio  $[\text{SDS}]/[\alpha\text{-CD}] \cong 0.52$ , where the 2:1 species represent a 78% of the inclusion complexes (see inset in Figure 2). As the temperature increases, that maximum moves slightly to higher molar ratios, and the percentage of 2:1 complexes decreases. Thus, at 308 K,  $[\alpha\text{-CD}_2\text{SDS}_1]$  goes to its maximum value at  $[\text{SDS}]/[\alpha\text{-CD}] \cong 0.57$ , where the 2:1 species represent a 46% of the inclusion complexes. The population analysis shows that less than 10% of the inclusion complexes have 1:1 stoichiometry for  $[\text{SDS}]/[\alpha\text{-CD}] < 0.33$  and  $T = 283$  K, which should be taken into account for the design of applications lying on  $\text{CD}_2\text{SDS}_1$  complexes as building units.<sup>4–7</sup>

**$\beta$ -Cyclodextrin.** Figure 3 shows the binding isotherms collected for this system at eight different temperatures between 283 and 323 K. The results are clearly different from those obtained with  $\alpha\text{-CD}$  in that the recorded heat is much lower for  $\beta\text{-}$  than for  $\alpha\text{-CD}$  and no positive heat could be detected in the whole range of temperatures and concentration ratios studied. As with  $\alpha\text{-CD}$ , an inflection point is present at all temperatures, although it appears at higher concentration ratios ( $\sim 0.8$ ). The SBS model fitted satisfactorily the isotherms with four parameters accounting for  $\beta\text{-CD}_1\text{SDS}_1$  and  $\beta\text{-CD}_2\text{SDS}_1$  as the complex species in solution. As before, the six-parameter try was useful to discard the existence of 1:2 species, agreeing again with the findings from MD simulations (see Table 4).<sup>20</sup> The quality of the fits is shown in Figure 3, and the parameters are given in Table 3. The thermodynamic parameters for the formation of the  $\beta\text{-CD}_1\text{SDS}_1$  complex are close to those furnished by the SSIS model (see Figures S3B and S3C in the Supporting Information), indicating that the calorimetric signal is dominated by the formation of the 1:1 complex. In fact, the system shows an unambiguous negative cooperativity ( $K_{21} \ll K_{11}/4$ ), with a temperature-independent Hill slope at half saturation in the range [0.5, 0.6]. Contrary to

**Table 3. Thermodynamic Parameters for the Binding of SDS with the Three Native CDs, Obtained by Fitting Calorimetric Data with the Sequential Binding Sites (SBS) Model (Eq 1)<sup>a,b,c</sup>**

	<i>T</i> (K)	10 <sup>−3</sup> <i>K</i> <sub>11</sub> (M <sup>−1</sup> )	10 <sup>−3</sup> <i>K</i> <sub>ij</sub> (M <sup>−1</sup> )	Δ <i>H</i> <sub>11</sub> <sup>o</sup> (kJ/mol)	Δ <i>H</i> <sub>ij</sub> <sup>o</sup> (kJ/mol)	<i>T</i> Δ <i>S</i> <sub>11</sub> <sup>o</sup> (kJ/mol)	<i>T</i> Δ <i>S</i> <sub>ij</sub> <sup>o</sup> (kJ/mol)	Δ <i>G</i> <sub>11</sub> <sup>o</sup> (kJ/mol)	Δ <i>G</i> <sub>ij</sub> <sup>o</sup> (kJ/mol)	10 <sup>11</sup> χ <sup>2</sup> (J <sup>2</sup> )
α-CD	283.15	40.8 ± 0.7	58 ± 1	−20.2 ± 0.2	−62.1 ± 0.2	4.8 ± 0.2	−36.2 ± 0.2	−24.98 ± 0.04	−25.83 ± 0.04	7.3
	288.15	43.9 ± 0.4	35.1 ± 0.3	−25.52 ± 0.07	−61.08 ± 0.05	0.07 ± 0.07	−36.02 ± 0.05	−25.60 ± 0.02	−25.06 ± 0.02	4.4
	293.15	43.9 ± 0.7	22.3 ± 0.2	−29.65 ± 0.06	−60.49 ± 0.06	−3.61 ± 0.07	−36.10 ± 0.07	−26.04 ± 0.04	−24.39 ± 0.02	1.7
	298.15	28.2 ± 0.3	15.8 ± 0.2	−30.66 ± 0.04	−62.23 ± 0.07	−5.27 ± 0.04	−38.27 ± 0.07	−25.39 ± 0.02	−23.96 ± 0.03	6.4
	303.15	30.2 ± 0.7	10.0 ± 0.3	−35.19 ± 0.06	−59.5 ± 0.4	−9.20 ± 0.08	−36.3 ± 0.4	−25.99 ± 0.05	−23.21 ± 0.09	25
	308.15	23.3 ± 0.1	6.74 ± 0.06	−37.65 ± 0.03	−58.2 ± 0.2	−11.90 ± 0.03	−35.7 ± 0.2	−25.75 ± 0.01	−22.57 ± 0.02	4.3
β-CD	283.15	24 ± 2	0.6 ± 0.2	−3.55 ± 0.04	−3 ± 1	20.2 ± 0.2	12 ± 1	−23.7 ± 0.2	−14.9 ± 0.7	0.059
	288.15	24.2 ± 0.1	0.63 ± 0.03	−6.235 ± 0.004	−1.2 ± 0.2	17.94 ± 0.01	14.2 ± 0.2	−24.17 ± 0.01	−15.4 ± 0.1	0.23
	293.15	22.8 ± 0.1	0.89 ± 0.03	−9.179 ± 0.005	0.60 ± 0.08	15.27 ± 0.01	17.1 ± 0.1	−24.45 ± 0.01	−16.54 ± 0.08	0.36
	298.15	20.8 <sup>d</sup> ± 0.1	0.777 <sup>d</sup> ± 0.03	−11.950 <sup>d</sup> ± 0.008	2.02 <sup>d</sup> ± 0.07	12.69 ± 0.01	18.5 ± 0.1	−24.64 ± 0.01	−16.5 ± 0.1	0.58
	303.15	18.56 ± 0.02	0.506 ± 0.005	−14.856 ± 0.003	4.37 ± 0.01	9.904 ± 0.004	20.06 ± 0.03	−24.760 ± 0.002	−15.68 ± 0.03	0.48
	308.15	16.45 ± 0.03	0.61 ± 0.01	−18.350 ± 0.004	7.54 ± 0.06	6.510 ± 0.006	23.98 ± 0.07	−24.860 ± 0.004	−16.43 ± 0.04	1.2
	313.15	17.9 ± 0.2	0.60 ± 0.05	−20.03 ± 0.02	4.9 ± 0.2	5.44 ± 0.04	21.5 ± 0.3	−25.48 ± 0.03	−16.6 ± 0.2	1.9
	318.15	15.40 ± 0.08	0.38 ± 0.02	−22.68 ± 0.01	6.3 ± 0.2	2.81 ± 0.02	22.0 ± 0.2	−25.49 ± 0.01	−15.7 ± 0.1	3.8
γ-CD	323.15	15.3 ± 0.1	0.61 ± 0.04	−24.97 ± 0.03	6.1 ± 0.3	0.91 ± 0.04	23.3 ± 0.3	−25.88 ± 0.03	−17.2 ± 0.2	13
	283.15	3.90 ± 0.05	1.36 ± 0.05	−9.12 ± 0.07	24.1 ± 0.4	10.34 ± 0.08	41.1 ± 0.5	−19.45 ± 0.03	−16.98 ± 0.09	0.45
	288.15	3.76 ± 0.02	0.70 ± 0.07	−8.50 ± 0.05	35 ± 4	11.21 ± 0.05	51 ± 4	−19.71 ± 0.01	−15.7 ± 0.2	0.64
	293.15	2.54 ± 0.01	0.53 ± 0.08	−9.28 ± 0.08	44 ± 6	9.82 ± 0.08	59 ± 6	−19.10 ± 0.01	−15.3 ± 0.4	0.36
	298.15	2.181 ± 0.008	0.78 ± 0.06	−9.46 ± 0.06	35 ± 1	9.58 ± 0.06	51 ± 1	−19.046 ± 0.009	−16.5 ± 0.2	0.19
	303.15	1.889 ± 0.005	0.40 ± 0.03	−8.26 ± 0.03	48 ± 2	10.74 ± 0.03	63 ± 2	−19.003 ± 0.007	−15.1 ± 0.2	0.097
	308.15	1.50 ± 0.01	0.32 ± 0.06	−7.78 ± 0.08	50 ± 4	10.94 ± 0.08	65 ± 4	−18.73 ± 0.02	−14.7 ± 0.5	0.13

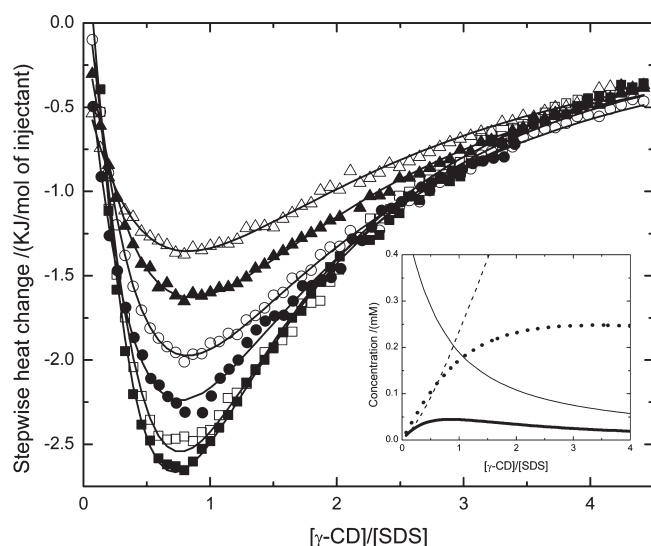
<sup>a</sup>  $T\Delta S^o = \Delta H^o - \Delta G^o$ ;  $\Delta G^o = -RT \ln K$ . <sup>b</sup> For α-CD and β-CD, the subscripts *ij* represent the CD<sub>2</sub>SDS<sub>1</sub> species, while in the case of γ-CD they stand for CD<sub>1</sub>SDS<sub>2</sub>. <sup>c</sup> In the last column, χ<sup>2</sup> stands for the global minimum of the objective function (eq 5) except for the case of β-CD at 283.15 K, where the global minimum has no physical meaning and a local one was taken. <sup>d</sup> To illustrate the importance of correcting for CD water content: If this were ignored, *K*<sub>11</sub> and *K*<sub>21</sub> would be 31.78 and 2.62 mM<sup>−1</sup>, respectively, whereas Δ*H*<sub>11</sub><sup>o</sup> = −10.46 kJ/mol and Δ*H*<sub>21</sub><sup>o</sup> = −0.69 kJ/mol.

Table 4. Relevant Microscopic Data Obtained by MD Simulation<sup>a</sup> for the Different Species at 298 K

	waters contacting SDS (total-head-tail) [SDS(1)/SDS(2)]	waters inside the CD [CD(1)/CD(2)]	SDS–H <sub>2</sub> O H-bonds [SDS(1)/SDS(2)]	CD–H <sub>2</sub> O H-bonds [CD(1)/CD(2)]	CD–SDS H-bonds [CD(1)/CD(2)] [SDS(1)/SDS(2)]	intramolecular CD H-bonds [CD(1)/CD(2)]	intermolecular CD–CD H-bonds
free SDS	29.8 ± 3.9 11.2 ± 1.8 22.4 ± 3.7		7.5 ± 1.3				
free CD							
α-CD		2.01 ± 0.92		33.0 ± 3.0		2.09 ± 0.82	
β-CD		6.1 ± 1.3		38.7 ± 3.7		1.66 ± 0.85	
γ-CD		13.0 ± 1.7		45.6 ± 3.6		2.19 ± 0.87	
Δ:†		0	3.0 ± 1.1	27.7 ± 2.9	2.50 ± 0.85	4.02 ± 0.93	
	18.4 ± 3.1 5.0 ± 1.5 13.5 ± 2.9 18.2 ± 2.9 7.5 ± 2.6 12.1 ± 2.8 19.1 ± 3.1 6.9 ± 2.7 13.4 ± 3.0 10.0 ± 2.1 5.8 ± 1.7 4.5 ± 1.7 9.4 ± 2.0 6.6 ± 1.6 3.8 ± 1.6 11.9 ± 2.6 6.0 ± 1.6 7.2 ± 2.3 8.4 ± 2.1 4.1 ± 1.3 4.3 ± 1.8 8.0 ± 2.0 4.6 ± 1.4 3.6 ± 1.7 10.7 ± 3.0 3.8 ± 1.6 8.3 ± 2.7	0.83 ± 0.94	5.0 ± 1.8 4.4 ± 1.9	32.7 ± 3.0	1.01 ± 0.81	5.1 ± 1.3	
β-CD							
γ-CD		5.7 ± 1.8		40.5 ± 3.3	1.9 ± 1.2	3.2 ± 1.1	
Δ∇:†		0	4.2 ± 1.2	18.1 ± 2.4	0.65 ± 0.83	5.84 ± 0.39	9.2 ± 1.6
α-CD		0.9 ± 1.0	4.4 ± 1.1	20.2 ± 2.3	1.33 ± 0.80	6.89 ± 0.34	10.5 ± 1.6
β-CD		1.26 ± 0.76					
γ-CD		5.0 ± 1.7	3.2 ± 1.6	33.1 ± 3.4	1.52 ± 0.83	4.81 ± 0.93	5.1 ± 1.7
ΔΔ:†		0	2.54 ± 0.93	22.8 ± 2.9	2.57 ± 0.80	4.0 ± 1.3	5.0 ± 2.3
α-CD		0.25 ± 0.51	1.0 ± 1.1	29.2 ± 3.1	2.13 ± 0.96	3.8 ± 1.1	4.1 ± 1.7
β-CD							
γ-CD		7.3 ± 2.0	5.1 ± 1.8	37.3 ± 3.8	1.17 ± 0.56	3.3 ± 1.1	3.7 ± 2.0
Δ:††		1.59 ± 0.98	5.0 ± 1.4	34.5 ± 3.0	1.08 ± 0.81	7.09 ± 0.92	
γ-CD	16.4 ± 2.9 7.4 ± 2.1 10.1 ± 2.7	16.6 ± 3.1 7.6 ± 2.1 10.3 ± 2.8					

<sup>a</sup>The methodology for the MD simulations is described in full detail in ref 20.





**Figure 4.** Integrated heat change per mole of injectant versus  $[\gamma\text{-CD}]/[\text{SDS}]$  molar ratio at 283 (■), 288 (□), 293 (●), 298 (○), 303 (▲), and 308 K (△). Inset: Concentration of free  $\gamma\text{-CD}$  (dashed thin line), free SDS (solid thin line),  $\gamma\text{-CD}_1\text{SDS}_1$  complexes (dotted thick line), and  $\gamma\text{-CD}_1\text{SDS}_2$  complexes (solid thick line) as a function of the  $[\gamma\text{-CD}]/[\text{SDS}]$  ratio, calculated from the isotherm at 283 K.

what happened for  $\{\alpha\text{-CD}+\text{SDS}\}$  systems, the relative uncertainty of  $K_{21}$  is much higher than that of  $K_{11}$  in all cases involving  $\beta\text{-CD}$  (see Figure S1). Between 283 and 323 K, the maximum  $[\beta\text{-CD}_2\text{SDS}_1]$  concentration occurs at a  $[\text{SDS}]/[\beta\text{-CD}]$  molar ratio in the range  $[0.57, 0.61]$ , moving slightly to higher ratios as the temperature increases. At this point, the 2:1 species represent around 11% of the inclusion complexes, regardless of the temperature (see inset in Figure 3), lying within the literature interval at 298 K (from less than 10% to 30%).<sup>52,69,76,79</sup> This runs into the rough view of  $\beta\text{-CD}_2\text{SDS}_1$  as the dominant species in solution when the  $[\text{SDS}]/[\beta\text{-CD}]$  molar ratio is 0.5.<sup>5</sup> From 283 to 323 K, the formation of 1:1 complexes goes from being governed by entropy to being controlled by enthalpy. The formation of the second-order complex is entropy-driven, as is usual in negatively cooperative systems. Brown<sup>103</sup> noted that this combination occurs when the first binding results in a loss of configurational entropy. This could be related to the appearance of kinks in the hosted chain fraction,<sup>20</sup> with the result that more  $\text{CH}_2$  groups are included in the  $\beta\text{-CD}$  cavity, thus making the 2:1 complex formation less likely. As noted above, this is revealed in Table 4 by a lowering of the SDS-tail hydration when going from  $\alpha\text{-CD}_1\text{SDS}_1$  to  $\beta\text{-CD}_1\text{SDS}_1$  complexes.

**$\gamma\text{-Cyclodextrin}$ .** Figure 4 displays the binding isotherms measured for this system at six temperatures between 283 and 308 K. The overall titration process is exothermic and the recorded heat even smaller than for  $\beta\text{-CD}$ . All of the isotherms exhibit a minimum that moves to higher molar ratios and decreases in magnitude as the temperature increases (the minimum values  $-2.6$  and  $-1.4 \text{ kJ mol}^{-1}$  are located at 0.8 and 0.9  $[\gamma\text{-CD}]/[\text{SDS}]$  molar ratios for 283 and 308 K, respectively). The minimization of the objective function is significantly worse (higher  $\chi^2$  values) when the  $\gamma\text{-CD}_1\text{SDS}_2$  species is not considered, meaning that at least this second-order complex coexists with the  $\gamma\text{-CD}_1\text{SDS}_1$  species. This is not surprising, given the wider cavity of  $\gamma\text{-CD}$  as compared to that of  $\alpha\text{-}$  and  $\beta\text{-CD}$ . Furthermore, molecular

dynamic simulations led unambiguously to the same conclusion (Table 4).<sup>20</sup> The six-parameter fit points to the possible existence of  $\gamma\text{-CD}_2\text{SDS}_1$  complexes, but it is not conclusive because, on the other hand, the reached global minima are flat and provide unrealistic parameters for four of the six isotherms. MD simulations pointed to the existence of these species too.<sup>20</sup> Moreover, the presence of  $\gamma\text{-CD}_2\text{SDS}_2$  species should not be discarded either.<sup>50</sup> However, only the thermodynamic characterization of 1:1 and 1:2 species is statistically justified with the available data. Figure 4 shows that the SBS model was able to reproduce very well the experimental results considering the coexistence of  $\gamma\text{-CD}_1\text{SDS}_1$  and  $\gamma\text{-CD}_1\text{SDS}_2$  complexes. As the temperature increases, the maximum  $[\gamma\text{-CD}_1\text{SDS}_2]$  is reached at increasing  $[\gamma\text{-CD}]/[\text{SDS}]$  molar ratios, from 0.90 at 283 K to 1.4 at 308 K. The percentage of 1:2 complexes at this point decreases from 21% at 283 K to 7% at 308 K (see inset in Figure 4). The fitted parameters are reported in Table 3. Note that  $\Delta H_{11}^\circ$  and  $\Delta H_{12}^\circ$  have opposite signs (the second-order complex formation is entropy driven), the calorimetric signal being dominated by  $\Delta H_{11}^\circ$ . The Hill slope at half saturation is insensitive to temperature changes and locates between 0.9 and 1.1. This constancy around unity would typically point to a scheme of noncooperative binding at identical sites, but the SSIS model was unable to describe the system behavior (see Appendix in the Supporting Information for more details). Freire and coauthors<sup>29</sup> pointed out that binding isotherms for a molecule with two identical and independent sites could be indistinguishable from those obtained for a molecule with two different binding sites exhibiting positive cooperativity. The latter option is consistent with the evident reduction of available space in the  $\gamma\text{-CD}$  cavity after the formation of the  $\gamma\text{-CD}_1\text{SDS}_1$  species, effectively yielding different binding site sizes for the first- and second-order formation processes.

**Comparison between the Results Obtained for the Three Cyclodextrins.** In general, the negative contributions to  $\Delta H_{ij}^\circ$  ( $i, j = 1, 2$ ) are attributed to a combination of three factors: the van der Waals interaction between the inner wall of the CD and the hydrocarbon chain of the surfactant, the release of high enthalpy water from the cyclodextrin cavity into bulk solution,<sup>37,104</sup> and, for the case of 2:1 complexes, the formation of CD–CD H-bonds, a contribution that is expected to be relatively weak because it is compensated by the breaking of H-bonds between CDs and water molecules. Note that the most negative  $\Delta H_{11}^\circ$  values are attained with  $\alpha\text{-CD}$ , due to the efficient expulsion of water molecules with very low coordination number<sup>105</sup> (Table 4) and to the close host–guest contact favored by the small diameter of the  $\alpha\text{-CD}$  cavity. For the same reason,  $\Delta H_{21}^\circ$  values are very large and negative only for this cyclodextrin (Table 3). The most positive  $\Delta H_{ij}^\circ$  values correspond to the formation of  $\gamma\text{-CD}_1\text{SDS}_2$  complexes, presumably due to the electrostatic repulsion of the two anionic SDS heads.<sup>20</sup> Regarding  $\Delta S_{ij}^\circ$  ( $i, j = 1, 2$ ), three main contributions are usually considered,<sup>37,41</sup> the van der Waals interaction between the alkyl chain of the guest and the inner wall of the CD cavity, the conformational changes of that alkyl chain, and the release of “high energy” and “low entropy”<sup>41</sup> water molecules from the CD cavity and around the alkyl chain of the guest during the complex formation process. The first and second contributions are usually negative because they imply loss of guest molecule rotational and translational degrees of freedom, while the third is positive.<sup>104</sup> The close fit between SDS and  $\alpha\text{-CD}$ , which favors both their mutual interaction and the all-trans conformation adopted by the

hosted SDS-tail fraction,<sup>20</sup> explains the negative values of  $\Delta S_{11}^\circ$  and  $\Delta S_{21}^\circ$  in  $\alpha$ -CD:SDS complexes. On the contrary, these quantities are positive for  $\beta$ - and  $\gamma$ -CD:SDS complexes at all of the studied temperatures due to the higher number of water molecules expelled from the CD cavity (Table 4),<sup>20</sup> to a weaker van der Waals interaction, and to the fact that the hosted SDS chain fraction is allowed to adopt gauche conformations.

**4.2. Heat Capacity Change of Binding.** Using the  $\Delta H^\circ$  values in Table 3, the heat capacity changes  $\Delta C_p^\circ = (\partial \Delta H^\circ / \partial T)_p$  for CD:SDS complexation were obtained and are displayed in Table 5. To our knowledge, these are the first  $\Delta C_p^\circ$  values reported for CD:SDS mixtures. Considering the  $T$  range and the number of single temperatures employed in the ITC measurements, these  $\Delta C_p^\circ$  values are considered to be reliable.

Because of its relation with entropy changes ( $\Delta C_p^\circ = T(\partial \Delta S^\circ / \partial T)_p$ ), heat capacity changes are a measure of the temperature variation of organization or order in the system,<sup>106–108</sup> placing  $\Delta C_p^\circ$  as a particularly relevant property to study the formation of inclusion complexes. For this quantity, efforts have been made to quantitatively evaluate the above-mentioned contributions (i)–(iv) (see introduction to section 4) from thermodynamic data, relying on schemes that try to isolate each of them,<sup>109</sup> but this route requires a big experimental effort and remains to be a complicated endeavor. Attempts have also been made to estimate in an indirect manner contributions (v) and (vi) for  $\Delta C_p^\circ$ ,<sup>110</sup> but a direct assessment of the importance of the last one is missing. This gap is filled in this section, using the  $\Delta C_p^\circ$  values in Table 5 and MD simulations results.

For hydrophobic substances, such as benzene, toluene, and short  $n$ -alkanes, the heat capacity change for the transfer from its pure state to water is positive,<sup>111</sup> indicating that solute dehydration gives rise to  $\Delta C_p^\circ < 0$ . Stemming from this result, the negative  $\Delta C_p^\circ$  values obtained for the formation of inclusion complexes (1:1 stoichiometry) between amphiphilic molecules and cyclodextrins<sup>109,112</sup> have been interpreted as due to the dehydration of the nonpolar section of the amphiphilic guest when it places itself inside the CD cavity. Dehydration has also been invoked to understand  $\Delta C_p^\circ < 0$  for the formation of complexes formed between proteins and carbohydrates,<sup>113,114</sup> whose contact surfaces are devoid of water when binding occurs. It appears that the negative  $\Delta C_p^\circ$  values in Table 5 for the formation of  $\alpha$ -CD<sub>1</sub>SDS<sub>1</sub> and  $\beta$ -CD<sub>1</sub>SDS<sub>1</sub> complexes with SDS are caused to a great extent by dehydration, a process that the MD simulations showed not only to involve the hydrocarbon chain of SDS but also its polar head (Table 4).<sup>20</sup> The fact that for the  $\gamma$ -CD<sub>1</sub>SDS<sub>1</sub> complex  $\Delta C_p^\circ$  is positive and small illustrates that for  $\gamma$ -CD none of the contributions (i)–(vi) is dominant, but rather they balance each other. This, in turn, can be traced to the differences found on the molecular level events leading to those contributions (see Table 4) for  $\gamma$ -CD:SDS complexes as compared to those formed with  $\alpha$ -CD and  $\beta$ -CD.

For the process where either a CD molecule or a SDS molecule is incorporated to a 1:1 complex to form the  $\alpha$ -CD<sub>2</sub>-SDS<sub>1</sub>,  $\beta$ -CD<sub>2</sub>SDS<sub>1</sub>, and  $\gamma$ -CD<sub>1</sub>SDS<sub>2</sub> complexes, Table 5 indicates that  $\Delta C_p^\circ > 0$ . Hence, the dominating negative contribution to  $\Delta C_p^\circ$  due to dehydration (for  $\alpha$ -CD and  $\beta$ -CD) is counterbalanced by another large and positive contribution, which is also revealed in the  $\gamma$ -CD case. It is our contention that conformational changes of the CD upon complexation contribute significantly to this positive  $\Delta C_p^\circ$ . Given that a positive  $\Delta C_p^\circ$  is associated with an order-formation process,<sup>109</sup> this contribution

**Table 5. Calculated Values of the Heat Capacity Change of Binding<sup>a</sup>**

	$\Delta C_{p,11}^\circ$ , kJ/(mol K)	$\Delta C_{p,ij}^\circ$ , kJ/(mol K)
$\alpha$ -CD	$-0.67 \pm 0.06$	$0.13 \pm 0.05$
$\beta$ -CD	$-0.54 \pm 0.01$	$0.24 \pm 0.04$
$\gamma$ -CD	$0.04 \pm 0.03$	$0.9 \pm 0.3$

<sup>a</sup> For  $\alpha$ -CD and  $\beta$ -CD, the subscripts  $ij$  represent the CD<sub>2</sub>SDS<sub>1</sub> species, while in the case of  $\gamma$ -CD they stand for CD<sub>1</sub>SDS<sub>2</sub>.

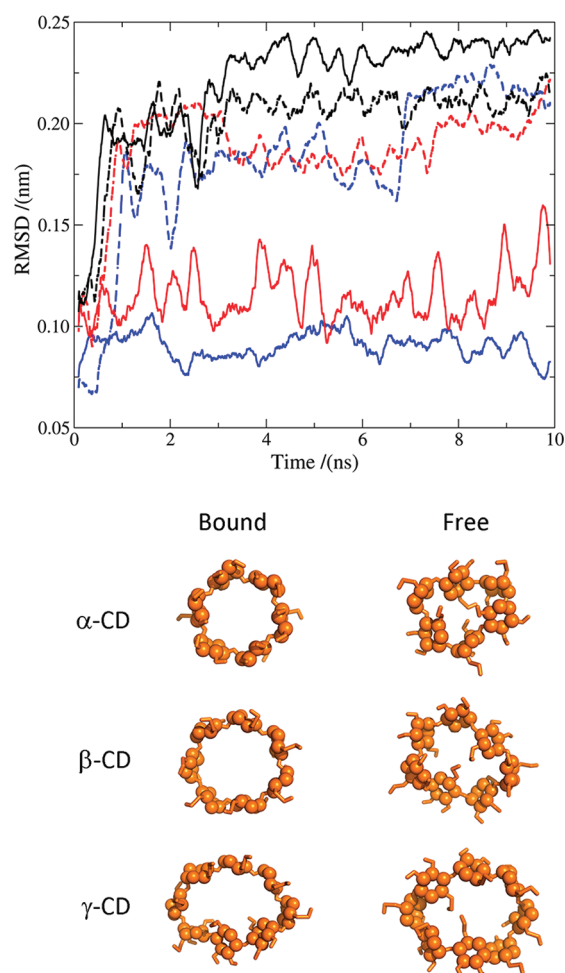


**Figure 5.** Top: Root mean square deviations of  $\alpha$ - (blue),  $\beta$ - (red), and  $\gamma$ - (black) cyclodextrins as a function of time, obtained from molecular dynamics simulations performed at 323 K. The initial structures were preformed CD<sub>2</sub>SDS<sub>1</sub> complexes from which one of the CDs fell apart within the first 3 ns. The solid and dashed lines correspond to the CD that remained threaded by one SDS molecule and to the CD that left the complex, respectively. The crystal structures of the cyclodextrins (PDB entries: 1BTC, 3CGT, 1D3C) were used as a reference to determine the rmsd values. The methodology for the MD simulations is described in full detail in ref 20. Bottom: Representative structures for the bound and free  $\alpha$ -,  $\beta$ -, and  $\gamma$ -CDs in aqueous solution, corresponding to the final conformations of the trajectories employed to calculate the rmsd.

refers to the process where a “flexible” CD molecule becomes “tight”. Because MD simulations can provide support or disregard this hypothesis, root-mean-square deviations (rmsd) of  $\alpha$ -,  $\beta$ -, and  $\gamma$ -CD using their respective crystal structures as reference were obtained as a function of time (10 ns) at 323 K,

the results being displayed in Figure 5. For each cyclodextrin, the starting structure was a  $\text{CD}_2\text{SDS}_1$  complex, from which one CD fell apart within the first 3 ns.<sup>20</sup> The free and threaded cyclodextrins follow uncorrelated trajectories in the range [7, 10] ns. From the comparison of the rmsd, it is inferred that the threading of  $\alpha$ - or  $\beta$ -CD by one hydrocarbon chain increases the structural order of the cyclodextrin. Figure 5 also indicates that the magnitude of the conformational changes suffered by the cyclodextrin upon threading decreases from  $\alpha$ -CD to  $\beta$ -CD, with  $\gamma$ -CD being a borderline case. It is worth noting (Figure 5, bottom right) that the three free CD structures are stabilized in solution by H-bonds between opposite side hydroxyls that, in the case of  $\gamma$ -CD, produce a more cyclic structure as compared to the threaded cyclodextrin. In summary, it appears that the conformational changes of the CD molecules upon binding are in fact an important contribution to the thermodynamics of CD:SDS inclusion complexes. Such contribution is enhanced in the second-order complex formation process either by the threading of a second hydrocarbon chain (the case of  $\gamma\text{-CD}_1\text{SDS}_2$ ) or by the intermolecular CD–CD H-bonds that stabilize the structure (the case of  $\alpha\text{-CD}_2\text{SDS}_1$  and  $\beta\text{-CD}_2\text{SDS}_1$  complexes), as well as by an increase of the (lateral) intramolecular CD H-bonds (Table 4).<sup>20</sup>

## 5. CONCLUSIONS

A detailed and critical review of the reported binding constants for CD:SDS inclusion complexes has been performed, handling a 41-paper database and using the categorization of experimental techniques made by Mwakibete et al.<sup>19</sup> as starting point. This review, together with the experience gained in the experimental, model application, and interpretation parts of the present work, allow us to suggest three technique-related and three model-related recommendations to obtain reliable association parameters for CD-based inclusion complexes: (i) the cyclodextrin water content should not be ignored, (ii) low sensitivity techniques and operation in a short-range of concentration ratios should be avoided, (iii) overlapping of additional processes that could screen the target signal, like solute aggregation phenomena, should be taken to a minimum in the experiment design and, if any, explicitly considered in the data analysis, (iv) the employed model should consider the possible existence of second-order complexes, (v) oversimplified approaches neglecting the equilibrium concentration of any species should be discarded, and (vi) speculative assumptions concerning binding site features should be avoided<sup>29</sup> by preferring in the first instance macroscopic (overall or stepwise) to site (intrinsic) binding constants.

A multiple-temperature ITC study of CD:SDS complexes was carried out, leading to the first reported heat capacity changes of binding for these systems. Observance of the recommendation (iv) was guaranteed by the employment of a model that allows for the simultaneous presence of 1:1, 1:2, and 2:1 species. Its software implementation using the simulated annealing algorithm yielded the accurate determination of the thermodynamic parameters. Our homemade program has improved versatility and convergence to the global minimum when compared to commercial software. An additional advantage is that the populations of every species at any temperature and nominal concentration of the solutes are also calculated, information that might be useful for the design of new materials based on the self-assembly of a specific complex.<sup>4–7</sup> As for the complex stoichiometry, the present ITC analysis and earlier MD simulations<sup>20</sup> led to the same conclusion,

that the species  $\alpha\text{-CD}_2\text{SDS}_1$ ,  $\beta\text{-CD}_2\text{SDS}_1$ , and  $\gamma\text{-CD}_1\text{SDS}_2$  coexist with their respective first-order species, while the occurrence of  $\gamma\text{-CD}_2\text{SDS}_1$  complexes remains uncertain.

An interesting feature of the second-order complexes for  $\beta$ - and  $\gamma$ -CD is that their formation is entropy-driven, in contrast with the corresponding first-order complex formation processes, which are governed by both enthalpy and entropy. In the case of  $\alpha$ -CD, both mechanisms are enthalpy-driven at  $T > 283$  K. Microscopic data from earlier MD simulations<sup>20</sup> have proved to be very useful to assist the discussion on the free energy contributions. Moreover, MD simulation results played a key role in assessing a significant contribution to the positive heat capacity changes characterizing the formation of  $\alpha\text{-CD}_2\text{SDS}_1$ ,  $\beta\text{-CD}_2\text{SDS}_1$ , and  $\gamma\text{-CD}_1\text{SDS}_2$  complexes, which is that due to the conformational changes of CD molecules upon binding.

$\alpha$ -CD:SDS systems were found to be positively cooperative, with increasing Hill slope as  $T$  decreases. On the contrary,  $\beta$ -CD:SDS and  $\gamma$ -CD:SDS systems display temperature-independent Hill slopes that are consistent with negative cooperativity and with different binding sites exhibiting positive cooperativity, respectively. This assorted behavior, together with the current critical revision of published data, implies that the inclusion complexes of the three native CDs with SDS are good candidates to test any technique intended to furnish reliable binding constants.

## ■ ASSOCIATED CONTENT

**S Supporting Information.** Figures S1 and S2 and appendix (containing Figure S3), where the  $\beta$ -CD:SDS isotherms are analyzed with the SSIS model after a brief reminder of its bases. This material is available free of charge via the Internet at <http://pubs.acs.org>.

## ■ AUTHOR INFORMATION

### Corresponding Author

\*E-mail: [angel.pineiro@usc.es](mailto:angel.pineiro@usc.es) (Á.P.); [costasmi@unam.mx](mailto:costasmi@unam.mx) (M.C.).

### Present Addresses

<sup>S</sup>Department of Chemical Engineering, University of California, Santa Barbara, California 93106, United States.

<sup>||</sup>Laboratori de Medicina Computacional, Unitat de Bioestadística, Facultat de Medicina, Universitat Autònoma de Barcelona, E-08193 Bellaterra, Barcelona, Spain.

## ■ ACKNOWLEDGMENT

This work was supported by grants 99844-Q from CONA-CyT-México, IN104210 from PAPIIT-DGAPA-UNAM, MAT2011-25501 from MICINN-Spain, and INCITE08PXIB206050PR from XUGA-Spain. Á.P. thanks “Xunta de Galicia” for his “Isidro Parga Pondal” research position. We are grateful to the “Centro de Supercomputación de Galicia” (CESGA) for the computing time used to perform the MD simulations related to Table 4 and Figure 5.

## ■ REFERENCES

- (1) Del Valle, E. M. M. *Process Biochem.* **2004**, 39, 1033–1046.
- (2) Szejtli, J. *Chem. Rev.* **1998**, 98, 1743–1754.
- (3) Challa, R.; Ahuja, A.; Ali, J.; Khar, R. K. *AAPS PharmSciTech* **2005**, 6, E329–E357.



- (4) Hernández-Pascacio, J.; Garza, C.; Banquy, X.; Díaz-Vergara, N.; Amigo, A.; Ramos, S.; Castillo, R.; Costas, M.; Piñeiro, Á. *J. Phys. Chem. B* **2007**, *111*, 12625–12630.
- (5) Jiang, L.; Peng, Y.; Yan, Y.; Deng, M.; Wang, Y.; Huang, J. *Soft Matter* **2010**, *6*, 1731–1736.
- (6) Jiang, L.; Peng, Y.; Yan, Y.; Huang, J. *Soft Matter* **2011**, *7*, 1726–1731.
- (7) Jiang, L.; Yan, Y.; Huang, J. *Adv. Colloid Interface Sci.* **2011**, *169*, 13–25.
- (8) dos Santos, J. R.; Couceiro, R.; Concheiro, A.; Torres-Labandeira, J.; Alvarez-Lorenzo, C. *Acta Biomater.* **2008**, *4*, 745–755.
- (9) Cesteros, L. C.; González-Teresa, R.; Katime, I. *Eur. Polym. J.* **2009**, *45*, 674–679.
- (10) Lu, Q.; Chen, D.; Jiao, X. *Chem. Mater.* **2005**, *17*, 4168–4173.
- (11) Bibby, A.; Mercier, L. *Green Chem.* **2003**, *5*, 15–19.
- (12) Bissell, R. A.; Córdova, E.; Kaifer, A. E.; Stoddart, J. F. *Nature* **1994**, *369*, 133–137.
- (13) Harada, A. *Acc. Chem. Res.* **2001**, *34*, 456–464.
- (14) Ogoshi, T.; Harada, A. *Sensors* **2008**, *8*, 4961–4982.
- (15) Miyake, K.; Yasuda, S.; Harada, A.; Sumaoka, J.; Komiyama, M.; Shigekawa, H. *J. Am. Chem. Soc.* **2003**, *125*, 5080–5085.
- (16) Eisenberg, B. *Proc. Natl. Acad. Sci. U.S.A.* **2008**, *105*, 6211–6212.
- (17) Li, W.; Claridge, T. D. W.; Li, Q.; Wormald, M. R.; Davis, B. G.; Bayley, H. *J. Am. Chem. Soc.* **2011**, *133*, 1987–2001.
- (18) Hernández-Pascacio, J.; Banquy, X.; Pérez-Casas, S.; Costas, M.; Amigo, A.; Piñeiro, Á. *J. Colloid Interface Sci.* **2008**, *328*, 391–395.
- (19) Mwakibete, H.; Cristantino, R.; Bloor, D. M.; Wyn-Jones, E.; Holzwarth, J. F. *Langmuir* **1995**, *11*, 57–60.
- (20) Brocos, P.; Díaz-Vergara, N.; Banquy, X.; Pérez-Casas, S.; Costas, M.; Piñeiro, Á. *J. Phys. Chem. B* **2010**, *114*, 12455–12467.
- (21) Wiseman, T.; Williston, S.; Brandts, J. F.; Lin, L.-N. *Anal. Biochem.* **1989**, *179*, 131–137.
- (22) Paula, S.; Sues, W.; Tuchtenhagen, J.; Blume, A. *J. Phys. Chem.* **1995**, *99*, 11742–11751.
- (23) Junquera, E.; Peña, L.; Aicart, E. *J. Solution Chem.* **1994**, *23*, 421–430.
- (24) Connors, K. A. *Binding Constants: The Measurement of Molecular Complex Stability*; John Wiley & Sons: New York, 1987; Chapter 2.
- (25) Sackett, D. L.; Saroff, H. A. *FEBS Lett.* **1996**, *397*, 1–6.
- (26) Klotz, I. M.; Walker, F. M.; Pivan, R. B. *J. Am. Chem. Soc.* **1946**, *68*, 1486–1490.
- (27) Indyk, L.; Fisher, H. F. Theoretical aspects of isothermal titration calorimetry. In *Methods in Enzymology*; Ackers, G. K., Johnson, M. L., Eds.; Academic Press: New York, 1998; Vol. 295, pp 350–364.
- (28) *ITC Data Analysis in Origin. Tutorial Guide*; MicroCal, LLC: Northampton, U.S., 2004.
- (29) Freire, E.; Schön, A.; Velazquez-Campoy, A. Isothermal titration calorimetry: General formalism using binding polynomials. In *Methods in Enzymology*; Johnson, M. L., Holt, J. M., Ackers, G. K., Eds.; Academic Press: San Diego, CA, 2009; Vol. 455, pp 127–155.
- (30) Piñeiro, Á.; Banquy, X.; Pérez-Casas, S.; Tovar, E.; García, A.; Villa, A.; Amigo, A.; Mark, A. E.; Costas, M. *J. Phys. Chem. B* **2007**, *111*, 4383–4392.
- (31) Press, W. H.; Teukolsky, S. A.; Vetterling, W. T.; Flannery, B. P. *Numerical Recipes in C++. The Art of Scientific Computing*; Cambridge University Press: Cambridge, UK, 2002.
- (32) Okubo, T.; Kitano, H.; Ise, N. *J. Phys. Chem.* **1976**, *80*, 2661–2664.
- (33) Kitano, H.; Okubo, T. *J. Chem. Soc., Perkin Trans. 2* **1977**, 432–435.
- (34) Satake, I.; Ikenoue, T.; Takeshita, T.; Hayakawa, K.; Maeda, T. *Bull. Chem. Soc. Jpn.* **1985**, *58*, 2746–2750.
- (35) Hersey, A.; Robinson, B. H.; Kelly, H. C. *J. Chem. Soc., Faraday Trans. 1* **1986**, *82*, 1271–1287.
- (36) Palepu, R.; Reinsborough, V. C. *Can. J. Chem.* **1988**, *66*, 325–328.
- (37) Okubo, T.; Maeda, Y.; Kitano, H. *J. Phys. Chem.* **1989**, *93*, 3721–3723.
- (38) Saint Aman, E.; Serve, D. *J. Colloid Interface Sci.* **1990**, *138*, 365–375.
- (39) Sehgal, P.; Sharma, M.; Wimmer, R.; Larsen, K. L.; Otzen, D. E. *Colloid Polym. Sci.* **2006**, *284*, 916–926.
- (40) Wan Yunus, W. M. Z.; Taylor, J.; Bloor, D. M.; Hall, D. G.; Wyn-Jones, E. *J. Phys. Chem.* **1992**, *96*, 8979–8982.
- (41) Turco Liveri, V.; Cavallaro, G.; Giammona, G.; Pitarresi, G.; Puglisi, G.; Ventura, C. *Thermochim. Acta* **1992**, *199*, 125–132.
- (42) Ikeda, T.; Ooya, T.; Yui, N. *Polym. Adv. Technol.* **2000**, *11*, 830–836.
- (43) Liao, D.; Dai, S.; Tam, K. C. *J. Rheol.* **2009**, *53*, 293–308.
- (44) Al-Sherbini, E. A. M. *Colloids Surf., A* **2009**, *352*, 1–4.
- (45) Liu, Y.; Liu, Y.; Guo, R. *J. Colloid Interface Sci.* **2010**, *351*, 180–189.
- (46) Sehgal, P.; Sharma, M.; Larsen, K. L.; Wimmer, R.; Doe, H.; Otzen, D. E. *J. Dispersion Sci. Technol.* **2008**, *29*, 885–890.
- (47) Gray, J. E.; Maclean, S. A.; Reinsborough, V. C. *Aust. J. Chem.* **1995**, *48*, 551–556.
- (48) Satake, I.; Yoshida, S.; Hayakawa, K.; Maeda, T.; Kusumoto, Y. *Bull. Chem. Soc. Jpn.* **1986**, *59*, 3991–3993.
- (49) Georges, J.; Desmettre, S. J. *Colloid Interface Sci.* **1987**, *118*, 192–200.
- (50) Funasaki, N.; Yodo, H.; Hada, S.; Neya, S. *Bull. Chem. Soc. Jpn.* **1992**, *65*, 1323–1330.
- (51) Dharmawardana, U. R.; Christian, S. D.; Tucker, E. E.; Taylor, R. W.; Scamehorn, J. F. *Langmuir* **1993**, *9*, 2258–2263.
- (52) Junquera, E.; Tardajos, G.; Aicart, E. *Langmuir* **1993**, *9*, 1213–1219.
- (53) Guo, Q. X.; Li, Z. Z.; Ren, T.; Zhu, X. Q.; Liu, Y. C. *J. Inclusion Phenom. Mol. Recognit. Chem.* **1994**, *17*, 149–156.
- (54) García-Río, L.; Leis, J. R.; Mejuto, J. C.; Pérez-Juste, J. J. *J. Phys. Chem. B* **1997**, *101*, 7383–7389.
- (55) Yin, B.; Sang, Q.; Wei, X.; Sun, D. *Riyong Huaxue Gongye* **2001**, *31*, 1–3.
- (56) Bo, T.; Xu, W.; Jing, W.; Chengguang, Y.; Zhenzhen, C.; Yi, D. *J. Phys. Chem. B* **2006**, *110*, 8877–8884.
- (57) García-Río, L.; Méndez, M.; Paleo, M. R.; Sardina, F. J. *J. Phys. Chem. B* **2007**, *111*, 12756–12764.
- (58) Xing, H.; Lin, S.; Yan, P.; Xiao, J.; Chen, Y. *J. Phys. Chem. B* **2007**, *111*, 8089–8095.
- (59) Sehgal, P.; Sharma, M.; Larsen, K. L.; Wimmer, R.; Otzen, D. E.; Doe, H. *J. Dispersion Sci. Technol.* **2008**, *29*, 128–133.
- (60) Jiang, L.; Deng, M.; Wang, Y.; Liang, D.; Yan, Y.; Huang, J. *J. Phys. Chem. B* **2009**, *113*, 7498–7504.
- (61) Bendazzoli, C.; Mileo, E.; Lucarini, M.; Olmo, S.; Cavrini, V.; Gotti, R. *Microchim. Acta* **2010**, *171*, 23–31.
- (62) Park, J. W.; Song, H. J. *J. Phys. Chem.* **1989**, *93*, 6454–6458.
- (63) Sasaki, K. J.; Christian, S. D.; Tucker, E. E. *Fluid Phase Equilib.* **1989**, *49*, 281–289.
- (64) Sasaki, K. J.; Christian, S. D.; Tucker, E. E. *J. Colloid Interface Sci.* **1990**, *134*, 412–416.
- (65) Wilson, L. D.; Siddall, S. R.; Verrall, R. E. *Can. J. Chem.* **1997**, *75*, 927–933.
- (66) Shen, X.; Belletete, M.; Durocher, G. *Langmuir* **1997**, *13*, 5830–5836.
- (67) Zhu, X.; Xu, X.; Lin, B.; Wenz, G.; Wehrle, S. *Gaodeng Xuexiao Huaxue Xuebao* **1998**, *19*, 1504–1506.
- (68) Eli, W.; Chen, W.; Xue, Q. *J. Chem. Thermodyn.* **1999**, *31*, 1283–1296.
- (69) Lin, C.; Huang, H.; Chen, H. *J. Chromatogr., A* **2001**, *917*, 297–310.
- (70) Guernelli, S.; Laganà, M. F.; Mezzina, E.; Ferroni, F.; Siani, G.; Spinelli, D. *Eur. J. Org. Chem.* **2003**, 4765–4776.
- (71) Wintgens, V.; Amiel, C. *J. Photochem. Photobiol., A* **2004**, *168*, 217–226.
- (72) Jiang, L.; Yan, Y.; Huang, J.; Yu, C.; Jin, C.; Deng, M.; Wang, Y. *J. Phys. Chem. B* **2010**, *114*, 2165–2174.
- (73) Rekharsky, M. V.; Inoue, Y. *Chem. Rev.* **1998**, *98*, 1875–1918.
- (74) Bellini, M. S.; Deyl, Z.; Manetto, G.; Kohlícková, M. *J. Chromatogr., A* **2001**, *924*, 483–491.

- (75) Crisantino, R.; De Lisi, R.; Milioto, S.; Pellerito, A. *Langmuir* **1996**, *12*, 890–901.
- (76) Milioto, S.; Bakshi, M. S.; Crisantino, R.; De Lisi, R. *J. Solution Chem.* **1995**, *24*, 103–120.
- (77) Otzen, D. E.; Oliveberg, M. *J. Mol. Biol.* **2001**, *313*, 479–483.
- (78) Xing, H.; Xiao, J. *J. Dispersion Sci. Technol.* **2009**, *30*, 27–32.
- (79) Retna Raj, C.; Ramaraj, R. *Electrochim. Acta* **1998**, *44*, 279–285.
- (80) Tsianou, M.; Alexandridis, P. *Langmuir* **1999**, *15*, 8105–8112.
- (81) Poghosyan, A. H.; Arsenyan, L. H.; Gharabekyan, H. H.; Koetz, J.; Shahinyan, A. A. *J. Phys. Chem. B* **2009**, *113*, 1303–1310.
- (82) Wilson, L. D.; Verrall, R. E. *Can. J. Chem.* **1998**, *76*, 25–34.
- (83) Connors, K. A. *Chem. Rev.* **1997**, *97*, 1325–1357.
- (84) Pistolis, G.; Malliaris, A. *Chem. Phys. Lett.* **1999**, *303*, 334–340.
- (85) Pistolis, G.; Malliaris, A. *Chem. Phys. Lett.* **1999**, *310*, 501–507.
- (86) Xu, Y.; Bolisetty, S.; Ballauff, M.; Müller, A. H. E. *J. Am. Chem. Soc.* **2009**, *131*, 1640–1641.
- (87) García-Río, L.; Leis, J. R.; Mejuto, J. C.; Pérez-Juste, J. J. *Phys. Chem. B* **1998**, *102*, 4581–4587.
- (88) *Complex Formation*; Troy, D. B., Ed.; Remington: The Science and Practice of Pharmacy; Lippincott Williams & Wilkins: Baltimore, MD, 2005; pp 186–200.
- (89) Loftsson, T.; Hreinsdóttir, D.; Másson, M. *J. Inclusion Phenom. Macrocyclic Chem.* **2007**, *57*, 545–552.
- (90) Loukas, Y. L. *Pharm. Sci.* **1997**, *3*, 343–346.
- (91) Amado, A. M.; Ribeiro-Claro, P. J. A. *J. Chem. Soc., Faraday Trans.* **1997**, *93*, 2387–2390.
- (92) Manor, P. C.; Saenger, W. *J. Am. Chem. Soc.* **1974**, *96*, 3630–3639.
- (93) Saenger, W.; Noltemeyer, M.; Manor, P. C.; Hingerty, B.; Klar, B. *Bioorg. Chem.* **1976**, *5*, 187–195.
- (94) Xing, H.; Zhou, H.; Yu, H.; Gou, Z.; Xiao, J. *J. Chem. Eng. Data* **2011**, *56*, 1423–1432.
- (95) Jiang, Y. B.; Wang, X. J. *Appl. Spectrosc.* **1994**, *48*, 1428–1431.
- (96) Xie, J. W.; Huang, D. S.; Xu, J. G.; Chen, G. Z. *Chin. Sci. Bull.* **1997**, *42*, 1468–1472.
- (97) Escandar, G. M.; de la Peña, A. M. *Appl. Spectrosc.* **2001**, *55*, 496–503.
- (98) Xing, H.; Lin, S.; Xiao, J. *J. Chem. Eng. Data* **2010**, *55*, 1940–1944.
- (99) Brittain, A. H.; Cox, A. P.; Duxbury, G.; Hersey, T. G.; Jones, R. G. *Mol. Phys.* **1972**, *24*, 843–851.
- (100) Hamai, S.; Sakurai, H. *J. Chromatogr., A* **1998**, *800*, 327–332.
- (101) Funasaki, N.; Ishikawa, S.; Neya, S. *J. Phys. Chem. B* **2004**, *108*, 9593–9598.
- (102) Hamai, S. *Bull. Chem. Soc. Jpn.* **1986**, *59*, 2979–2982.
- (103) Brown, A. *Int. J. Mol. Sci.* **2009**, *10*, 3457–3477.
- (104) Perry, C. S.; Charman, S. A.; Prankerd, R. J.; Chiu, F. C. K.; Scanlon, M. J.; Chalmers, D.; Charman, W. N. *J. Pharm. Sci.* **2006**, *95*, 146–158.
- (105) Pereira, C. S.; de Moura, A. F.; Freitas, L. C. G.; Lins, R. D. *J. Braz. Chem. Soc.* **2007**, *18*, 951–961.
- (106) Kronberg, B.; Patterson, D. *J. Chem. Soc., Faraday Trans. 1* **1981**, *77*, 1223–1235.
- (107) Pérez-Casas, S.; Castillo, R.; Costas, M. *J. Phys. Chem. B* **1997**, *101*, 7043–7054.
- (108) Costas, M.; Patterson, D. *Thermochim. Acta* **1987**, *120*, 161–181.
- (109) Olvera, Á.; Pérez-Casas, S.; Costas, M. *J. Phys. Chem. B* **2007**, *111*, 11497–11505.
- (110) Stödeman, M.; Gómez-Orellana, I.; Hallén, D. *J. Inclusion Phenom. Macrocyclic Chem.* **2003**, *46*, 125–132.
- (111) Makhatadze, G. I.; Privalov, P. L. *J. Chem. Thermodyn.* **1988**, *20*, 405–412.
- (112) Hallén, D.; Schön, A.; Shehatta, I.; Wadsö, I. *J. Chem. Soc., Faraday Trans.* **1992**, *88*, 2859–2863.
- (113) García-Hernández, E.; Zubillaga, R. A.; Chavelas-Adame, E. A.; Vázquez-Contreras, E.; Rojo-Domínguez, A.; Costas, M. *Protein Sci.* **2003**, *12*, 135–142.
- (114) Chavelas, E. A.; García-Hernández, E. *Biochem. J.* **2009**, *420*, 239–247.